Combined bulk-rock Lu-Hf and Sm-Nd isotopic study of Archean granitoids and mafic rocks from Sangmelima terranes (Ntem Complex, south Cameroon): Geodynamic implications

Joseph Martial Akame, Vinciane Debaille, Marc Poujol

Precambrian Research

Combined bulk-rock Lu-Hf and Sm-Nd isotopic study of Archean granitoids and mafic rocks from Sangmelima terranes (Ntem Complex, south Cameroon): Geodynamic implications.

--Manuscript Draft--

Manuscript Number:	PRECAM-D-22-00420R2
Article Type:	Research Paper
Keywords:	Hf isotopes; Nd isotopes; Archean granitoids; Congo Craton; Ntem Complex
Corresponding Author:	Joseph Martial AKAME, Dr Bruxelles, Bruxelles-Capitale BELGIUM
First Author:	Joseph Martial AKAME, Dr
Order of Authors:	Joseph Martial AKAME, Dr
	Vinciane DEBAILLE, Prof Dr
	Marc POUJOL, Prof. Dr
Abstract:	Hafnium and neodymium isotopes provide robust tool tracers for tracking the mechanisms of crustal generation and differentiation, from mantle extraction to the late geological processes undergone by the studied rocks. Though these two isotope systems commonly behave similarly and define a positive correlation between 143Nd/144Nd and 176Hf/177Hf referred to as the "terrestrial array", they may differ in terrains having a complex geological history, such as Archean cratons. This study presents the first combined whole-rock Hf and Nd isotopic analyses of Archean mafic and felsic igneous rocks from the Sangmelima terranes in the Ntem Complex (located in the Northwest of Congo Craton (NW CC) in southern Cameroon). It mainly consists of Mesoarchean charnockites and tonalite-trondhjemite-granodiorite (TTG) suites, greenstone belts, mafic enclaves or dykes, and potassic granitoids. Mesoarchean charnockite and TTG suites have subchondritic initial 176Hf/177Hf and 143Nd/144Nd ratios with a mean initial (suffix (i)) ε176Hf(i) and ε143Nd(i) of –3.30 ± 1.40 and –3.85 ± 0.65 (2SD) respectively, implying the involvement of Eo- to Paleoarchean components in their petrogenesis. The bulk rock initial Hf and Nd isotope compositions of the gabbro and gabbronorites are suprachondritic (ε176Hf(i) = +3.4 to +8.2; ε143Nd(i) = +0.9 to +1.6), indicate that they were derived from a depleted mantle source. Coupled with pre-existing data from the literature, these new Hf-Nd isotopic data indicate that two episodes of mantle-derived mafic magmatism in the Ntem Complex occurred during the Mesoarchean period (i.e., at ~ 3.1 and 2.86 billion years (Ga)). Neoarchean dolerite dykes show broadly chondritic to supra-chondritic ε176Hf(i) and ε143Nd(i) values of –0.28 to +4.53 and TCHUR ages of 2.74 – 2.76 Ga, suggesting the derivation of doleritic magma from a depleted mantle source with either none or limited crustal residence time. Considering other Archean domains of the NW CC, there were multi-stage magmatism events and crustal growth events occurred at ~3.75 – 3.31 Ga, ~3.26 – 3.0 Ga, ~2.92 – 2.85 Ga, and ~2.75 – 2.72 Ga from Eoarchean to Neoarchean in the NW Congo Craton.
Suggested Reviewers:	Hanika Rizo, Prof. Dr Associat Professor, Carleton University hanika.rizo@carleton.ca Hf and Nd isotopic specialiste
	Martin Whitehouse, Prof .Dr. Professor, Swedish Museum of Natural History martin.whitehouse@nrm.se Archean specialist geology Research in isotope geology and bedrock geology
	Kristoffer Szilas, Prof .Dr Associate Professor,, University of Copenhagen Department of Geosciences and Natural Resource Management

	krsz@ign.ku.dk Archean Geology and Isotopic geochemistry
	Jean-Paul Liégeois, Prof.Dr Senior Researchers, Royal Museum for Central Africa Jean-paul.liegeois@africamuseum.be Precambrian Geology of Congo Craton
	Richard Palin, Prof.Dr Associate Professor, University of Oxford Department of Earth Sciences richard.palin@earth.ox.ac.uk Precambrian geology
Response to Reviewers:	

Combined bulk-rock Lu-Hf and Sm-Nd isotopic study of Archean granitoids and mafic rocks from Sangmelima terranes (Ntem Complex, south Cameroon): Geodynamic implications.

Joseph Martial AKAME[1,*], Vinciane DEBAILLE[1], Marc POUJOL[2]

[1]Laboratoire G-Time Géochimie isotopique. Université libre de Bruxelles. 50, Av. F.D. Roosevelt,CP 160/02, B-1050 Brussels, Belgium.

[2]University of Rennes, CNRS, Géosciences Rennes-UMR 6118, F-35000, Rennes, France.

*now at University of Rennes 1, CNRS,Géosciences Rennes-UMR 6118, F-35000, Rennes, France. Correspondence: (akamejosephmartial@gmail.com)

Abstract

Hafnium and neodymium isotopes provide robust tool tracers for tracking the mechanisms of crustal generation and differentiation, from mantle extraction to the late geological processes undergone by the studied rocks. Though these two isotope systems commonly behave similarly and define a positive correlation between $^{143}Nd/^{144}Nd$ and $^{176}Hf/^{177}Hf$ referred to as the "terrestrial array", they may differ in terrains having a complex geological history, such as Archean cratons. This study presents the first combined whole-rock Hf and Nd isotopic analyses of Archean mafic and felsic igneous rocks from the Sangmelima terranes in the Ntem Complex (located in the Northwest of Congo Craton (NW CC) in southern Cameroon). It mainly consists of Mesoarchean charnockites and tonalite-trondhjemite-granodiorite (TTG) suites, greenstone belts, mafic enclaves or dykes, and potassic granitoids. Mesoarchean charnockite and TTG suites have subchondritic initial $^{176}Hf/^{177}Hf$ and $^{143}Nd/^{144}Nd$ ratios with a mean initial (suffix $_{(i)}$) $\varepsilon^{176}Hf_{(i)}$ and $\varepsilon^{143}Nd_{(i)}$ of –3.30 ± 1.40 and –3.85 ± 0.65 (2SD) respectively, implying the involvement of Eo- to Paleoarchean components in their petrogenesis. The bulk rock initial Hf and Nd isotope compositions of the gabbro and gabbronorites are suprachondritic ($\varepsilon^{176}Hf_{(i)}$ =

+3.4 to +8.2; $\varepsilon^{143}Nd_{(i)}$ = +0.9 to +1.6), indicate that they were derived from a depleted mantle source. Coupled with pre-existing data from the literature, these new Hf-Nd isotopic data indicate that two episodes of mantle-derived mafic magmatism in the Ntem Complex occurred during the Mesoarchean period (i.e., at ~ 3.1 and 2.86 billion years (Ga)). Neoarchean dolerite dykes show broadly chondritic to supra-chondritic $\varepsilon^{176}Hf_{(i)}$ and $\varepsilon^{143}Nd_{(i)}$ values of –0.28 to +4.53 and T_{CHUR} ages of 2.74 – 2.76 Ga, suggesting the derivation of doleritic magma from a depleted mantle source with either none or limited crustal residence time. Considering other Archean domains of the NW CC, there were multi-stage magmatism events and crustal growth events occurred at ~3.75 – 3.31 Ga, ~3.26 – 3.0 Ga, ~2.92 – 2.85 Ga, and ~2.75 – 2.72 Ga from Eoarchean to Neoarchean in the NW Congo Craton.

Keywords: Hf isotopes; Nd isotopes; Archean granitoids; Congo Craton; Ntem Complex

1. Introduction

Both long-lived ^{176}Lu–^{176}Hf and ^{147}Sm–^{143}Nd isotope systems are robust tools for tracking the mechanisms of crustal generation and differentiation, from mantle extraction to the late geological processes it recorded through time (DePaolo, 1981; McCulloch and Bennett, 1994; Vervoort and Blichert-Toft, 1999; Salerno et al., 2021). Moreover, parent-daughter Lu/Hf and Sm/Nd ratios exhibit congruent low-pressure melting relationships as the parents, Lu and Sm, are both less incompatible compared to the daughters, Hf and Nd. This implies lower Lu/Hf and Sm/Nd ratios in the depleted mantle and, conversely, higher ratios in the crustal reservoirs. In general, the two isotopic systems are coupled and define a positive correlation between $^{143}Nd/^{144}Nd$ and $^{176}Hf/^{177}Hf$ referred as the "terrestrial array" (Vervoort and Blichert-Toft, 1999; Vervoort et al., 2011). However, this analogous geochemical behavior of these isotopic systems may diverge, especially in ancient terrains like Archean cratons that generally have undergone a long-lasting complex geologic history (e.g., Caro et al., 2005; Rizo et al., 2011; Vervoort,

2014; Hammerli et al., 2019; Salerno et al., 2021). It has been suggested that the decoupling of Nd and Hf isotopes resulted from the generation of Ca- and Mg-enriched bridgmanite residues in the deep mantle during the solidification of the early magma ocean (Caro et al., 2005; Rizo et al., 2011). Recent work suggests that consumption reactions and recrystallisation of REE-bearing accessory minerals such as apatite, allanite and titanite during high-grade metamorphism may induce disturbance of the Sm−Nd and Lu-Hf isotopic systems of the bulk rock (Hammerli et al., 2014, 2019; Fisher et al., 2020; Hammerli and Kemp, 2021; Salerno et al., 2021). Thus, investigating the behaviour of both isotopic systems in the older rocks in different cratons may not only improve the understanding of the origin of the decoupling of Lu-Hf and Sm-Nd isotopic systems, but also to better constrain early Earth evolution and differentiation processes.

Archean cratons represent only 15% of outcropping ancient terrain worldwide (Goodwin, 1981) and are the primordial archives that support our understanding of the Earth's early history. They mainly consists of the tonalite-trondhjemite-granodiorite (TTG) suite, charnockites, potassic granites (e.g., Martin, 1986) and greenstone belts which are dominantly composed of ultramafic to mafic volcanic sequences with associated sedimentary rocks (e.g., Smithies et al., 2018), variably metamorphosed up to amphibolite facies (Condie, 1994; de Wit and Ashwal, 1995; Sproule et al., 2002; Furnes et al., 2015). Of granitoids, TTG suites represents the ancient archetypal juvenile felsic component of Archean terrains (Smithies, 2000; Moyen and Martin, 2012 and references therein), and their decreasing occurrence in late Archean time with the progressive increase of the potassic granitoids indicate a significant geodynamic change on the Earth (Laurent et al., 2014; Halla et al., 2017; Cawood et al., 2018). Thus, studying and characterising the setting of TTG suites, their transition to potassic granitoids, and associated Archean mafic rocks is thus crucial to understand the differentiation and accretion mechanisms of Earth´s earliest crust. Numerous models suggest that the TTG suites are the product of the

partial melting of earlier mafic rocks of the Earth's crust in subduction zone settings (Condie, 1986; Martin, 1987; Moyen and Martin, 2012; Hoffmann et al., 2014). The episodic nature of TTG magmatism (i.e., at 3.80 billion years (Ga), 3.44 Ga, 3.33 Ga, 2.70 Ga) is, however, not compatible with the continuous character of modern subduction zone processes (Debaille et al., 2013; Martin et al., 2014). To add complexity, the parental magmas, presumably representing the first crust, are often no longer found on the terrestrial surface. The onset of the Archean continental crust may consequently mask a complex history of crustal reworking, concealing the nature of the most ancient crust on Earth.

In the present study, we performed the first combined bulk-rock Lu-Hf and Sm-Nd isotope analyses on Mesoarchean rocks from the Sangmelima terranes (Cameroon) located within the north-western margin of the Congo Craton (NW CC) (Fig.1). We aimed to characterize both the mantle sources and crustal components involved in the petrogenesis of the Archean crust in this important portion of the Congo craton. We also evaluate how much post-magmatic process affected the Hf and Nd isotope systems, and finally discuss the tectono-magmatic evolution of the NW Congo Craton with geodynamic implication of the Archean continental crustal growth models.

Fig.1

2. Geological background and samples

The Northwest Congo Craton (NW CC), in the west-central part of the African continent, covers the region of equatorial Africa that extends from the Republic of Congo to the Atlantic Ocean (Fig.1). It consists of three Archean domains, the Ntem Complex in southern Cameroon, the Monts de Cristal–North Gabonese Massif domain and Chaillu Massif in southern Gabon, surrounded by Proterozoic Orogenic Belts (e.g., Maurizot et al., 1986; Caen-Vachette et al., 1988; Toteu et al., 1994; Feybesse et al., 1998; Tchameni et al., 2000; Shang et al., 2004a; Chombong and Suh, 2013; Takam et al., 2009; de Wit and Linol, 2015; Thiéblemont et al.,

2018; Akame et al., 2020a). Eighty-five percent of the Archean basement rocks in the Ntem Complex are Mesoarchean rocks (e.g., Akame et al., 2020 end reference therein), which are dominated by ~3.15 – 2.85 Ga deformed and metamorphosed charnockites, TTGs and plutonic rocks, and minor supracrustal rocks (Tchameni et al., 2004; Chombong and Suh, 2013; Takam et al., 2009; Tchameni et al., 2010; Li et al., 2016; Akame et al., 2020a, 2021). The formation age of the greenstone belts remains poorly defined but probably falls in a period between 2.85 and 3.04 Ga (Tchameni et al., 2004; Chombong and Suh, 2013). Paleoarchean charnockite in the Ntem Complex has been dated at 3266 ± 5 million years (Ma) (SHRIMP zircon U-Pb; Takam et al., 2009). Nevertheless, this old crystallisation age of charnockites is usually considered as an inherited age (Li et al., 2016; Akame et al., 2020a). Amphibolite enclaves and gabbro dykes within the TTG suites were dated at 2862 ± 10 Ma (Li et al., 2016) and 2866 ± 6 Ma (Akame et al., 2020a), respectively. Neoarchean granitoids are composed of monzogranite and syenogranite, and were generated at two main age peaks of ~2.75 Ga and ~2.68 Ga (Tchameni et al., 2000; Akame et al., 2020a). The granitic-gneissic basement and greenstones belts were intruded by Neoarchean dolerite dykes at 2.72 Ga (Shang et al., 2007).

Structural, metamorphic and geochronological data from the Ntem Complex indicate the prominence of two ductile high-grade tectonothermal events at ~2.84 – 2.82 Ga and ~2.78 – 2.74 Ga (Maurizot et al., 1986; Tchameni et al., 2010; Akame et al., 2020a, 2020b, 2021). The Mesoarchean high-temperature metamorphism and the migmatisation of TTGs was contemporaneous with the regional penetrative deformation (referred as D1), while the Neoarchean event is related to the folding of S_1 regional foliation, development of C_2 shear zones and minor intrusions of anatectic origin (Akame et al., 2020a, 2020b, 2021).

The samples analysed in this paper were collected during fieldwork in the Sangmelima granite-greenstone terrane (SGB) outcropping in the northern part of the Ntem Complex (Fig. 1a). These 16 samples were previously studied by Akame et al. (2020a), who presented whole-

rock geochemical (Fig. 2, Table 1) and LA-ICP-MS zircon U−Pb data. Detailed field observations and a petrographic description of our sample set, including six mafic rocks (4 gabbronorites, 2 dolerites) and 10 granitoids, are provided in Akame et al. (2020a). At outcrops, Mesoarchean gabbronorite (ca. 2866 Ma) occurs either as monolithic enclaves of centimetre to metre size (samples AJM11, AJM14, AJM17) or as larger (50–200 m) mafic dykes (samples AJM16 ~ 2866 Ma) enclosed in granitoids. The Mesoarchean granitoids include a charnockitic suite (ca. 2850 – 2912 Ma) and a TTG suite (ca. 2865–2870 Ma). Neoarchean high-K granites (AJM25) and dolerite dykes (ca. 2723 Ma; AJM3, AJM 6), in most cases, are intrusive veins/dykes within charnockites and TTG. Uranium-Pb dating of zircons from the charnockites, TTG and granites indicates that the granitoids of the Ntem Complex were emplaced between 3050 Ma and 2750 Ma (Takam et al., 2009; Tchameni et al., 2010; Li et al., 2016; Akame et al., 2020a, 2021). In general, although there is a prominence of charnockites at ~2.91 Ga, TTG at ~2.87 Ga and granites at ~2.75 Ga, all three rock types can be found emplaced during those three Meso-Neoarchean events. Moreover, amphibolite and gabbro crystallisation at ~ 2.86 Ga was synchronous with the TTG magmatism in the Ntem Complex (Li et al., 2016; Akame et al., 2020a). Three samples (AJM10, AJM7, AJM16) analysed in this study are part of the series of samples on which zircon U-Pb ages have been previously determined (Akame et al., 2020a). Accordingly, the emplacement ages of the samples are also constrained.

Fig. 2

Table 1

3. Methods

Hafnium and Nd isotopic analyses of the 16 Mesoarchean samples of the Sangmelima area were conducted in the Laboratoire G-Time at Université libre de Bruxelles (ULB), Belgium. Around ~ 200 mg of whole rock powder of different samples were dissolved in a 1:3 mixture of subboiled concentrated HF and HNO_3. After 2 days on a hot plate at 120 °C, the supernatant

was removed, and the residues were placed in Parr high-pressure vessels at 150 °C for 48h using fresh acids in the same proportion. All the samples were recombined, dried out and re-dissolved using 12N HCl. A 5% aliquot was removed from the initial dissolution and spiked using ^{150}Sm–^{148}Nd and ^{175}Lu–^{179}Hf spikes. Hf and Rare Earth Elements (REE) were first purified using cationic resin. Hf was collected first in 1.5N HCl and REE were eluted in 6N HCl. For both spiked and unspiked cuts, the REE were further separated using HDEHP resin by increasing the HCl molarity. For both spiked and unspiked Hf cuts, first, Fe was removed from the matrix using an anionic column in HCl 6N. Then, Hf was purified from Ti on Ln–Spec resin using a mixture of HCl 6N and H_2O_2, while Hf was collected in 4N HF. Hafnium, Lu, Sm and Nd spiked cuts and Hf and Nd unspiked cuts were analysed at ULB on the HR–MC–ICP–MS Nu–Plasma 2 coupled to an Aridus dessolvator, using 0.05N HNO_3 plus traces of HF for Hf measurements. Hafnium isotopic ratios were corrected for mass fractionation by internal normalisation to the value of ^{179}Hf/^{177}Hf = 0.7325, and by bracketing every 2 samples with the JMC-475 standard, and the standard value of 0.282160 ± 0.000010 was used for subsequent correction (Blichert-Toft, 2001). Analyses of JMC475 yielded an external reproducibility of 68 ppm (2SD, n = 16). Two analyses of the USGS BHVO-2 geostandard gave an average ^{176}Hf/^{177}Hf ratio of 0.283111 ± 9 (2SD) in agreement with the value of ^{176}Hf/^{177}Hf = 0.283105 ± 11 reported by Weis et al. (2007). Neodymium isotope compositions were corrected for mass fractionation by internal normalisation to the value of ^{146}Nd/^{144}Nd = 0.7219, and the Rennes Nd standard was measured every two samples. The accepted value of ^{143}Nd/^{144}Nd = 0.511961 for the Rennes standard was used for subsequent corrections (Chauvel and Blichert-Toft, 2001). The repeated measurements of the Rennes Nd Standard gave an external reproducibility of 59 ppm (2SD, n = 19). Two analyses of the BHVO-2 geostandard gave an average ^{143}Nd/^{144}Nd ratio of 0.512975 ± 10 (2SD) in agreement with the value of ^{143}Nd/^{144}Nd = 0.512981 ± 10 reported by Weis et al. (2007). Spiked sample data were deconvolved following the procedure

of Debaille et al. (2007). Epsilon Nd and Hf values were calculated using the chondritic (CHUR) values of $^{143}Nd/^{144}Nd = 0.512630$;$^{147}Sm/^{144}Nd = 0.1960$; $^{176}Hf/^{177}Hf = 0.282785$ and $^{176}Lu/^{177}Hf = 0.0336$ (Bouvier et al., 2008). The Nd and Hf depleted mantle model ages (T_{DM}) were calculated using the following depleted mantle values: $^{143}Nd/^{144}Nd = 0.513150$ and $^{147}Sm/^{144}Nd = 0.2137$ (Goldstein et al., 1984), and $^{176}Hf/^{177}Hf = 0.283294$ and $^{176}Lu/^{177}Hf = 0.03933$ (Blichert-Toft and Puchtel, 2010). Isochrons were calculated with the ISOPLOT program (Ludwig, 2012), using the decay constants $\lambda^{176}Lu = 1.867 \times 10^{-11}\ yr^{-1}$, $\lambda^{147}Sm = 6.54 \times 10^{-12}\ yr^{-1}$.

4. Results

Whole rock ^{176}Lu–^{176}Hf and ^{147}Sm–^{143}Nd data for the Sangmelima felsic and mafic rocks are presented in Table 2. The $\varepsilon^{176}Hf$ and $\varepsilon^{143}Nd$ initial values (subscript i later) have been calculated at 2900 Ma for charnockites, 2870 Ma for TTGs and 2866 Ma for gabbronorites (Tchameni et al., 2010; Li et al., 2016; Akame et al., 2020a). For the Neoarchean potassic granite and dolerite dykes, the initial εHf and εNd have been calculated at 2750 Ma (Akame et al., 2020a) and 2723 Ma (Shang et al., 2007), respectively.

Table 2.

The Lu–Hf and Sm–Nd isotope data of the charnockites define errochrons corresponding to 3397 ± 88 Ma (MSWD = 0.068, n = 3) and 2443 ± 77 Ma (MSWD = 3.8, n = 3), respectively, Fig. 3a-b; Tables 2). The charnockite samples show individual $\varepsilon^{176}Hf_{(i)}$ and $\varepsilon^{143}Nd_{(i)}$ values that are all negative (from −4.1 to −1.4 for $\varepsilon Hf_{(i)}$ and −4.2 to −1.9 for $\varepsilon Nd_{(i)}$), except for sample AJM20 with a very negative $\varepsilon^{143}Nd_{(i)}$ value of −54 (Table 2). The $f_{Lu/Hf}$ factor ($f_{Lu/Hf} = [(^{176}Lu/^{177}Hf)_{sample}/(^{176}Lu/^{177}Hf)_{CHUR}] - 1$) varies between −0.7955 and −0.9272 (average $f_{Lu/Hf} = -0.8745$) whereas the $f_{Sm/Nd}$ factor ($f_{Sm/Nd} = [(^{147}Sm/^{144}Nd)_{sample}/(^{147}Sm/^{144}Nd)_{CHUR}] - 1$) ranges from 0.2882 to − 0.6213 with an average of −0.3058 (Table 2). They yielded T_{DM}(Hf) of 3317

to 3224 Ma (average = 3283 ± 6 Ma, 2SD), T_{DM}(Nd) of 3456 to 3196 Ma (average = 3355 ± 370 Ma, 2SD; without sample AJM20, Table 2).

Fig.3

The Mesoarchean TTG suites, including granodiorites and tonalitic gneisses, give ^{176}Lu-^{176}Hf and ^{147}Sm-^{143}Nd errochronous ages of 3539 ± 220 Ma ($^{176}Hf/^{177}Hf_{(i)}$ = 0.280687 ± 0.000035, MSWD = 8.9, n = 4) and 2661 ± 760 Ma ($^{143}Nd/^{144}Nd_{(i)}$ = 0.508840 ± 0.000480, MSWD = 23; n = 4), respectively (Fig. 3c-b). They have individual negative values $\varepsilon^{176}Hf_{(i)}$ of −7.4 to −0.9 and $\varepsilon^{143}Nd_{(i)}$ values of −3.3 to −5.1 (Table 2). Their $f_{Lu/Hf}$ factor varies from −0.5803 to −0.9463, whereas f_{Sm-Nd} factors are scattered between −0.4283 and −0.5695 (Table 2). All Mesoarchean tonalite-granodiorite samples yield T_{DM}(Nd) of 3284 to 3513 Ma with an average of 3366 ± 84 Ma (MSWD = 22; n = 6) and show T_{DM}(Hf) ages of 3172 to 3428 Ma with an average of 3312 ± 110 Ma (MSWD = 42; n = 6) (Table 2). The tonalitic gneisses display higher Lu/Hf and Sm/Nd ratios (Lu/Hf = 0.0436 – 0.0989 and Sm/Nd = 0.1404 – 0.1852) than the granodiorites (Lu/Hf = 0.0126 – 0.0216 and Sm/Nd = 0.1394 – 0.1572). The 2.75-Ga-old potassic granite (sample AJM25) cutting across TTG has subchondritic initial $^{176}Hf/^{177}Hf$ and $^{143}Nd/^{144}Nd$ ratios, with $\varepsilon^{176}Hf_{(i)}$ = –3.7 and $\varepsilon^{143}Nd_{(i)}$ = –4.6. These results correspond to T_{DM}(Hf) and T_{DM}(Nd) model ages of 3224 Ma and 3249 Ma, respectively (Table 2).

The whole rock Lu-Hf and Sm-Nd isotope data of all gabbronorite samples define errochrons corresponding to 3225 ± 1400 Ma (MSWD = 21; n = 4) and 3324 ± 1300 Ma (MSWD=14; n = 4), respectively, with $^{176}Hf/^{177}Hf_{(i)}$ of 0.28082 ± 0.00084 and $^{143}Nd/^{144}Nd_{(i)}$ of 0.508300 ± 0.001700 (Fig. 3e-f; Tables 2). All samples have high $^{176}Hf/^{177}Hf$ ratios (0.282396 – 0.283022), corresponding to positive $\varepsilon^{176}Hf_{(i)}$ values (+3.4 to +8.2) (Table 2), whereas the $^{143}Nd/^{144}Nd$ ratios range from $\varepsilon^{143}Nd_{(i)}$ values ranging from –2.3 to +1.6 (Table 2). They have $f_{Lu/Hf}$ factors of –0.2616 to +0.0320 and $f_{Sm/Nd}$ factor of –0.1969 to +0.0581. Their ranges of T_{DM}(Hf) and T_{DM}(Nd) model ages are 2634 to 3212 Ma and 3673 to 6118 Ma, respectively.

225 The Neoarchean dolerites have variable $\varepsilon^{143}Nd_{(i)}$ (–0.1 to +4.5) and $\varepsilon^{176}Hf_{(i)}$ (–0.3 to +16)
226 (Table 2). However, the factors $f_{Sm/Nd}$ and f_{Lu-Hf} show less scattered values, from –0.2935 to –
227 0.3046 and –0.6423 to –0.7127, respectively (Table 2). Their T_{DM}(Hf) of 2.27 to 3.09 Ga and
228 T_{DM}(Nd) of 2.66 to 3.12 Ga model ages are younger than those of the Neoarchean potassic
229 granite. Compared to the Mesoarchean gabbronorites, the range of the Lu/Hf ratio is limited,
230 between 0.068 – 0.084 and is lower (average 0.076).

231 Fig.3

232 **5. Discussion**

233 **5.1. Post-magmatic process and its effects on Hf-Nd radiogenic isotope systematics**

234 The Ntem complex underwent two major tectonothermal events between 2.84 and 2.74 Ga
235 (Akame et al., 2020a, 2020b, 2021). Consequently, it is necessary to assess the potential effect
236 of high-grade metamorphism and partial melting on the primary isotopic compositions of the
237 Sangmelima igneous rocks before undertaking any petrogenetic and geodynamic interpretation.
238 The gabbronorite and gabbro exhibit granoblastic textures and show granulite-facies
239 assemblage of orthopyroxene, clinopyroxene, biotite, plagioclase and amphibole (Fig S1). Most
240 of studied mafic and granitoid gabbronorite samples show low loss on ignition (LOI) values
241 (LOI < 3 wt%), which point to very limited post-crystallisation alteration effects. To evaluate
242 the element mobility during metamorphism, we plotted selected trace elements (REEs, Ti, Nb,
243 Ta, U, Y, Th, Cs, Rb, Pb, Sr and Hf) against Zr, one of the most immobile elements (Fig. 4 and
244 Fig. S2) (Polat and Hofmann, 2003). Rare earth elements (REEs) and most of high field strength
245 elements (HFSEs, e.g., Hf, Nb, Ta, and Ti), Sr and Y show positive correlation with Zr, and Ce
246 anomalies are absent (Ce/Ce*= 0.94 – 1.02), indicating that these elements were immobile
247 during metamorphism (Fig. S2) (Polat and Hofmann, 2003). The gabbronorite samples have
248 low Th (0.11 – 0.83ppm) and U (0.13 – 0.29 ppm) contents and Th/U ratio (0.82 – 3.68,
249 average = 1.76) similar to that of depleted MORB (Sun and McDonough, 1989), indicating
250 that Th and U were also immobile during metamorphism. Assessment of U and Th mobility is

difficult in the granitoids because of Pb loss. In contrast, some major large ion lithophile elements (LILEs, e.g. Cs, Rb, Ba and Pb) and K, show variable degrees of scatter against Zr (Fig. S3), suggesting that they have been modified by post-magmatic processes. The positive Tm anomaly for AJM19 is likely related to analytical artefacts (Fig. 2c-d) (Roth et al., 2018).

The ^{176}Lu–^{176}Hf and ^{147}Sm–^{143}Nd isotopic data of gabbronorite samples give errochronous ages of 3225 ± 1400 Ma and 3324 ± 1300 Ma, respectively (Fig. 3e-f), which are older than their emplacement age of ~2.87 Ga (Fig. 3e-f), suggesting that either these (1) samples are from a composite source, or (2) Hf-Nd isotopic systems were reset during metamorphism. In the chondrite-normalised REE diagrams (Fig. 2e; Anders and Grevesse, 1989a), most of gabbronorite samples show relatively consistent REE patterns that are similar to N-MORB (La_N/Yb_N = 0.82 – 0.98), except for one sample (AJM17) which show a clear LREE-enrichment (high La_N/Yb_N = 3.2 and low Sm/Nd = 0.25). This may suggest that the gabbronorite did not derive from a composite source, while the enrichment in LREE of sample AJM17 could reflect the accumulation of a LREE-rich phase like monazite, apatite titanite and allanite. However, the best explanation for LREE-enrichment is secondary alteration, as LREE are more mobile than HREE. One way to evaluate a possible mixing between two sources is to plot $^{176}Hf/^{177}Hf$ and $^{143}Nd/^{144}Nd$ against 1/Hf and 1/Nd (Shafer et al., 2010; Viehmann et al., 2018; Wainwright et al., 2019), as mixing is characterised by the alignment of the samples along a line in such a plot. Figure 5 shows that $^{176}Hf/^{177}Hf$ and $^{143}Nd/^{144}Nd$ ratios do not correlate with 1/Hf and 1/Nd, respectively (Fig. 5a-b), indicating that a mixing processes cannot account for the Hf–Nd errorchronous apparent ages observed for the Sangmelima gabbronorite. The L–Hf or Sm–Nd isotopic systems were possibly disturbed at the individual mineral scale. Samples AJM16 and AJM17 exhibit decoupled Hf-Nd isotopic compositions with $\varepsilon^{143}Nd_{(i)}$ value of −1.58 to −2.33 and $\varepsilon^{176}Hf_{(i)}$ of +3.37 to +8.25, and fall in the crustal contamination field (Fig. 4a; Hasenstab et al., 2021). However, crustal contamination and/or assimilation commonly

affect(s) both Lu-Hf and Sm-Nd isotope systems in mafic magmas (Nebel et al., 2014; Hasenstab et al., 2021). We therefore consider that the negative $\varepsilon^{143}Nd_{(i)}$ of samples AJM16 (−1.58 at 2870 Ma) and AJM17 (−2.33 at 2870 Ma) were likely resulting of post-crystallisation disturbance of the Sm-Nd isotope system. Hammerli et al. (2019) suggested that the formation or recrystallisation of REE-enriched minerals such as monazite, xenotime, apatite, allanite and epidote during metamorphism would alter the subsequent Nd isotope evolution of the rock by fractionation of their $^{147}Sm/^{144}Nd$ ratios. Following granulite-facies mineral assemblages and geochemical evidence for LREE-phase accumulation in sample AJM17, we suggest that their Sm–Nd systematics were more easily disturbed during the 2.84–2.84 Ma metamorphic event widely reported from the Sangmelima region (Shang et al., 2004a; Akame et al., 2020a, 2021). Monazite alteration with apatite corona in granodiorites hosting gabbro (sample AJM16) (Akame et al., 2021), suggests that recrystallisation of apatite (high Sm/Nd) and other Nd-bearing phases may have likely controlled the Nd isotopic composition of this rock. Collectively, the Sm−Nd isotope system of samples AJM16 and AJM17 does not represent the primary signature of their protolith, and they were disturbed during post-crystallisation process.

Two dolerite samples (AJM3, AJM6) show weathering texture such as chloritisation of biotite and sericitisation of plagioclase (Fig. S2), but moderate LOI values (2.32 – 2.80 wt%< 5), and show relatively uniform REE patterns (Fig. 2a-b), and no Ce/Ce* anomaly, indicating that REEs have not undergone significant modification (Polat and Hofmann, 2003). Sample AJM3 shows almost similar initial Nd and Hf isotopic values (−0.11 and −0.28, respectively), but in contrast sample AJM6 has a very high $\varepsilon^{176}Hf_{(i)}$ value (up to $\varepsilon^{176}Hf_{(i)}$ = +16.09) compared to the Sm−Nd isotope system with $\varepsilon^{143}Nd_{(i)}$ of +4.53. Considering that Hf might be remobilised in easily altered mafic rocks given the lack of robust phases (e.g. zircon) to anchor Hf or Lu (Hoffmann and Wilson, 2017), we suggest that the Lu-Hf system of this sample was disturbed during post-crystallisation processes. In addition, the Hf depleted model age of ca. 2270 Ma is

younger than the apparent emplacement age of 2723 ± 3 Ma (Shang et al., 2007), and does not overlap with any known magmatic or igneous event in the Sangmelima Terrane.

Most of the granitoid samples yield coherent $\varepsilon^{143}Nd_{(i)}$ and $\varepsilon^{176}Hf_{(i)}$ values ranging from −1.9 to −5.1 and −0.9 to −7.4, respectively (Table 2), whereas all but one Mesoarchean charnockite (AJM20) show very negative $\varepsilon^{143}Nd_{(i)}$ of −54.0 with no significant T_{DM}(Nd) age. Nevertheless, there is clearly a deviation from the trend in Hf, Nd isotope versus their parent/daughter ratios diagram and both isotopic systems give different "errorchron" ages (Figs. 3a-b, 3c-d). The lack of correlation between measured $^{143}Nd/^{144}Nd$-vs. 1/Nd, and $^{176}Hf/^{177}Hf$ vs. 1/Hf plots (Fig. 5a-b), suggests that the errorchrons are not an artefact of mixing (Fig. 5b), and may rather indicate the effects of different petrogenetic processes such as partial melting or melt segregation. For sample AJM20, the $\varepsilon^{143}Nd_{(i)}$ value of −54.0 suggests that the Sm–Nd isotopic systematics were substantially disturbed or reset possibly due to the breakdown of less-stable REE-rich accessory phases during the Mesoarchean high grade metamorphism events.

5.2. Hf - Nd isotopic signature and crustal growth

5.2.1. Granitoids

Shang et al. (2004a) studied the geochemical and Nd–Sr isotopic signatures of the Mesoarchean felsic rocks of the Sangmelima terranes and concluded that the primary magma of both charnockite and TTG suites derived from the similar late Paleoarchean eclogite facies basaltic proto-crust sources with contribution of a slightly enriched proto-crust. The Mesoarchean charnockites studied here are magnesian cordilleran-type granitoids (Akame et al., 2020a), and show Sr/Y ratio similar to those of Archean low to medium pressure TTG, which probably derived from partial melting of hydrous basalts (Moyen, 2011). Following the major and trace elements composition of the Sangmelima charnockites, Akame et al. (2020a) suggested that these rocks were likely formed by high degrees of partial melting of mafic rocks. Detailed geochemical studies (Akame et al., 2020a) have suggested that most of Mesoarchean

Sangmelima TTG suites are low to medium pressure TTGs that were probably generated by partial melting of enriched mafic rock and/or continental arc magma, possibly in a subduction zone. Both studies emphasise a contribution of a crustal component in the formation of the Sangmelima Mesoarchean granitoids.

The Mesoarchean charnockites and TTG suites we analysed have subchondritic $\varepsilon^{176}Hf_{(i)}$ (from −0.91. to −7.37 average of −3.3±1.4, n = 10) and $\varepsilon^{143}Nd_{(i)}$ (from –1.9 to –5.1, average of –3.85 ± 0.65, 2SD; n = 9) values (Fig. 5c-d). These subchondritic $\varepsilon^{143}Nd_{(i)}$ and $\varepsilon^{176}Hf_{(i)}$ values suggest either the involvement of significant crustal contamination or the involvement of a long-term Nd and Hf enriched component (relative to Sm and Lu) in these rocks. They reveal very similar T_{DM}(Hf) (3.22 − 3.32 Ga, average = 3.28 Ga and 3.17 − 3.43 Ga, average = 3.32 Ga, respectively) and T_{DM}(Nd) (3.19 – 3.45 Ga, average = 3.36 Ga and 3.28 – 3.51 Ga, average = 3.37 Ga, respectively), indicating that a proto-crust of ca. 3.2 – 3.5 Ga might have existed in the Sangmelima area. Li et al. (2016) reported zircon $\varepsilon^{176}Hf_{(i)}$ values between −1.3 and + 2.0 with an average of +0.0 for similar 2.92 Ga old charnockites from the Menguémé area, whereas a ca. 2.87 Ga Djoum trondhjemite displays $\varepsilon^{176}Hf_{(i)}$ between −2.0 and −6.1 with an average of −3.7, like the Sangmelima TTG suites. However, the zircon Lu-Hf model ages of ca. 3.3 – 3.5 Ga for the charnockite and 3.5 – 3.8 Ga for the trondhjemites (Li et al., 2016) are older than the whole rock T_{DM}(Hf) ages (3.17 – 3.43 Ga) calculated in this study. Nevertheless, the older whole-rock T_{DM}(Hf)age of 3.43 Ga overlap with the charnockite zircon T_{DM}(Hf). It is important to note that zircon Hf model age is usually calculated using a fixed Lu/Hf value that is supposed to represent the magmatic source of the zircon-hosting rocks (Amelin et al., 1999; Bodet and Schärer, 2000; Griffin et al., 2002; Iizuka et al., 2005; Kemp et al., 2007), but both elements may significantly be decoupled during intracrustal differentiation processes involving garnet or zircon, leading to spurious zircon T_{DM}(Hf) ages (Bea et al., 2018). In addition, Bea et al. (2018) suggested that using a single fixed Lu/Hf source value to calculate zircon T_{DM}(Hf) ages may

reflect the Lu/Hf heterogeneity of the source and lead to large overestimates of zircon T_{DM}(Hf) compare to whole-rock Hf or Nd model ages, notably in the case of zircons being much younger than their sources. Therefore, our new bulk-rock Lu−Hf isotope data combined with published zircon Hf data suggest the derivation of TTG magmas from an older enriched crustal reservoir, whereas the charnockite parental magmas evolved from a reservoir that was globally chondritic to enriched of Eo- to early Mesoarchean ages (~3.2 – 3.8 Ga).

Our new long-lived $^{147}Sm–^{143}Nd$ isotopic data ($\varepsilon^{143}Nd_{(i)}$= –1.9 to –5.1; Fig.5d) are consistent with published whole-rock $\varepsilon^{143}Nd_{(i)}$ from Sangmelima Mesoarchean granitoids (Shang et al., 2004a). The T_{DM}(Nd) model ages yield early Mesoarchean to Paleoarchean ages (ca. 3.20 – 3.52 Ga) for the samples studied, older than the inherited zircon U-Pb ages of 3057 ± 7 and 3155 ± 11Ma for the Sangmelima charnockites and TTG gneisses, respectively (Akame et al., 2020a). Pouclet et al. (2007) reported near chondritic $\varepsilon^{143}Nd_{(i)}$ values (–1.6 to +1.3) with an average of +0.8 and a T_{DM}(Nd) age around 2.92 – 3.10 Ga for Mesoarchean charnockites from the Ntem Complex. However, these Nd model ages (2.92 – 3.10 Ga) are younger than the 3057 – 3266 Ma ages of the oldest magmatic zircons dated in the granitoids from the Ntem complex (Takam et al., 2009; Akame et al., 2020a). In addition, some samples analysed in these previous studies were collected near or within the Nyong Paleoproterozoic Complex. Nevertheless, by recalculating the Nd isotopic data (using Bouvier et al. (2008) values for CHUR, 2.9 Ga for charnockites and 2.87 Ga for TTG suites crystallisation ages) from Shang et al. (2004a), it appears that the Sangmelima charnockites and TTGs have $\varepsilon^{143}Nd_{(i)}$ values of +0.16 to –5.63 (average = –2.14) and +0.50 to –5.07 (average = –2.17), respectively. Furthermore, Shang et al., (2004a) reported low $Sr_{(i)}$ ratios ranging from 0.70098 to 0.70314 at 2.85 Ga for the Sangmelima charnockitic and TTG suites. As a result, a local continental crust, extracted from the mantle between ~3200 and ~3520 Ma, probably played a significant role in the petrogenesis of the charnockites and TTGs from the Sangmelima terranes. This conclusion is consistent with

results of the whole-rock $\varepsilon^{176}Hf$ average of –3.3±1.4 for the same samples and consistent with a contribution of an ancient crustal component.

The chondritic zircon Hf signatures $\varepsilon^{176}Hf_{(i)} \sim 0$ for charnockite of Menguéme (Li et al., 2016) and near-chondritic whole-rock $\varepsilon^{143}Nd_{(i)}$ value of ~ +0.8 for charnockites reported by Pouclet et al. (2007), suggest that their chondritic signatures may reflect the formation of charnockite from sources evolving from a depleted mantle component that was formed earlier. However, both data reported by Li et al. (2016) including some zircons with superchondritic $\varepsilon^{176}Hf_{(i)}$ values ($\varepsilon^{176}Hf_{(i)} > 0$) and the positive whole-rock $\varepsilon^{143}Nd_{(i)}$ values reported by Pouclet et al. (2007) indicate that the Archean mantle of the Ntem Complex was partially depleted. The combined geochemical and isotopic (Sr, Nd, Hf and O) distinction between the charnockites and the TTG suites suggests that at least two different precursors, formed at different times, were involved in the petrogenesis of the Mesoarchean felsic rocks. The combination of the whole-rock Hf- and Nd model ages, as well as the data published by Shang et al. (2004a, re-calculated using the chondritic (CHUR) values of Bouvier et al. 2008; 2.90 Ga for charnockites, 2.87 for TTG suites and 2.75 Ga for high-K granites), suggest a progressive extraction during Eo- to-Mesoarchean ages (3750 – 3050Ma) with two major peaks evidenced by whole-rock T_{DM} ages of 3200 Ma and 3300 Ma of the protolith source of the Sangmelima charnockites and TTG magmas.

Fig.6

The high-K granite sample (AJM25) has higher K_2O/Na_2O (1.85), negative $\varepsilon^{176}Hf_{(i)}$ of –3.7 and $\varepsilon^{143}Nd_{(i)}$ of –4.6, consistent with their formation by partial melting of a LREE-enriched crustal source with a range in age from 3.22 to 3.24 Ga. These model ages (3.22 – 3.24 Ga) and isotopic signatures are slightly younger than those of some Mesoarchean granitoids of TTG composition (Table 2), that were formed by the melting of a mafic source. However, Na-enriched TTG do not produce melts that are sufficiently K_2O-rich to generate the high-K

granitoids (Watkins et al., 2007). Therefore, partial melting of relatively more K-rich components of this suite is required (eg. Patiño Douce and Beard, 1995). Our Hf-Nd isotopic data are consistent with the subchondritic Nd isotopic signatures ($\varepsilon^{143}Nd_{(i)}$ = –2.1 to –5.0, re-calculated at 2.75 Ga) reported by Shang et al. (2010), and the protolith emplacement age of the Sangmelima potassic granites at ca. >2.9 Ga (zircon U-Pb age ; Akame et al., 2020a).

5.2.2. Mafic rocks

Recently published zircon U−Pb dates show that most mafic rocks from the Ntem Complex were emplaced around 2866 – 2862 Ma (Li et al., 2016; Akame et al., 2020a), suggesting a significant episode of Mesoarchean mafic magmatism in this complex. Specifically, these are mafic assemblages within the Sangmelima terrane, such as the gabbronorite-gabbro assemblage (Akame et al., 2020a), and the amphibolites hosted in Djoum's TTG (Li et al., 2016), but also older garnet-bearing amphibolite (ca.3.1 Ga, Pb−Pb zircon evaporation age) from the Ebolowa supracrustal belt (Tchameni et al., 2004). The whole-rock $\varepsilon^{176}Hf_{(i)}$ values from the four gabbronorite and gabbro mafic samples from the Sangmelima terranes are positive, ranging from +3.4 to +8.2 with an average of ~ +5.9, which are overall close to the one of depleted mantle value of ~ +6.9 (Table 2). These values are broadly similar to those of the $\varepsilon^{176}Hf_{(i)}$ values (+0.1 to +4.8) for zircons from the 2.86 Ga amphibolite enclave in the trondhjemites (Fig.5c), (Li et al., 2016). Their $\varepsilon^{143}Nd_{(i)}$ values range from –2.3 to +4.5, indeed suggesting decoupled Hf- and Nd isotopic signatures. However, as mentioned above, the Nd isotopic compositions of the samples AJM16 and AJM17 were likely disturbed by post-magmatic processes such as metamorphism/metasomatism and/or by crustal contamination. Taking this effect into account, both unaltered samples (AJM11 and AJM14) have $\varepsilon^{143}Nd_{(i)}$ values of +0.9 to +1.6, which are similar to the $\varepsilon^{143}Nd_{(i)}$ values (+0.5 to +2.8) of ca. 3.1 Ga garnet-bearing amphibolites from the Ebolowa greenstone belt (Tchameni et al., 2004). Together with the published geochemical and isotopic data, we therefore suggest that the Ntem

Complex probably experienced two major Mesoarchean (~2.86 and ~3.1 Ga) episodes of juvenile mantle-derived mafic magmatism.

The whole-rock Sm–Nd and Lu–Hf data from the Neoarchean dolerite dykes yielded $\varepsilon^{143}Nd$ and $\varepsilon^{176}Hf$ values of –0.11 to +4.53 and –0.28 to +16.09, respectively, and are interpreted to be derived from depleted mantle reservoirs. However, the near-chondritic character ($\varepsilon^{143}Nd_{(i)}$ = –0.11 and $\varepsilon^{176}Hf_{(i)}$ = –0.28) with T_{DM}(Nd) of 3125 Ma and T_{DM}(Hf) of 3039 Ma for sample AJM3, and positive $\varepsilon^{143}Nd_{(i)}$ and $\varepsilon^{176}Hf_{(i)}$ values with model age of 2666 Ma and 2270 Ma may suggest distinct periods of dyke emplacement. Toteu et al. (1994) and Vicat et al. (1996) have suggested the existence of Eburnian doleritic magmatism in the Ntem Complex, but there are no geochronological data to support this assumption. We therefore consider that the Sangmelima dolerites are derived from a depleted mantle source, and the Lu−Hf isotopic system of sample AJM6 was probably disturbed during post-magmatic processes.

5.3. Geodynamic implications

The Ntem Complex is one of the largest Archean domains in southern Cameroon. The statistical zircon U–Pb and monazite U-Th-Pb ages of the igneous rocks from the Ntem Complex show that the Mesoarchean (2.92 – 2.85 Ga), with two major peaks at 2920 and 2866 Ma (Fig. 6), was an important period of magmatism (Takam et al., 2009; Tchameni et al., 2010; Chombong and Suh, 2013; Li et al., 2016; Akame et al., 2020a, 2021). This magmatism includes the widespread emplacement of charnockites, TTG suites and mafic igneous rocks (Li et al., 2016; Akame et al., 2020a), and the occurrence of minor dacite volcanism in the Mbalam greenstone belt (Chombong and Suh, 2013). Minor age peaks observed at 3.26 – 3.05 Ga have been interpreted as inherited ages of charnockites and TTG suites (Takam et al., 2009; Akame et al., 2020a). A few older xenocrystal zircons with ages of up to 3.3 Ga indicate the existence of early Meso-to Paleoarchean granitic crust in the Ntem Complex (Fig. 6). As proposed in the discussion on the Hf-Nd isotope compositions, the chondritic to subchondritic $\varepsilon^{143}Nd_{(i)}$ and

$\varepsilon^{176}Hf_{(i)}$ of Archean granitoids from the Ntem Complex point towards the involvement of ancient paleo-crust in their petrogenesis, rather than simple oceanic crust melting. They have whole-rock Hf-Nd and zircon T_{DM}(Hf) ages of ~3.9 – 3.0 Ga (Fig. 6), which may indicate the extraction of a mafic crust (without zircon) from the mantle (at ~3.9 – 3.25 Ga), followed by a first major recycling episode (at ~3.25 – 3.00 Ga) that produced the first felsic crust in the region. This ancient felsic crust is emphasised by the presence of inherited zircons of ~3.25 – 3.05 Ga in the granitoids (Takam et al., 2009; Akame et al., 2020a), and the formation of supracrustal rocks synchronous with the juvenile mantle-derived mafic magmatism dated at 3.14 – 3.07 Ga (Tchameni et al., 2004). The Lu−Hf and Sm−Nd isotopic data of 2.75 Ga high-K granite points to re-melting of Mesoarchean crustal material, whereas the 2.72 Ga dolerite magmas were extracted from mantle at ~ 2.74 – 2.76 Ga.

Fig.6

The geodynamic setting of the Archean Ntem Complex, in which significant Mesoarchean magmatism and metamorphism occurred, remains a subject of research and discussion. The emplacement of the widespread granitoids with associated mafic rocks may occur in various environments, including subduction-related tectonic settings (Shang et al., 2004a; Pouclet et al., 2007), a hotspot beneath the lithospheric mantle related to mantle plume activity (Li et al., 2016), or a subduction-accretionary geodynamic setting (Akame et al., 2020a). The latter alternative model was recently proposed to account for the formation of different lithological assemblages observed in the Ntem Complex from 3.2 to 2.75 Ga. Isotopic data published on the Archean basement rocks of the Ntem Complex (e.g. Tchameni et al., 2004; Shang et al., 2007; Li et al., 2016; Akame et al., 2020a) show that mafic and felsic magmatism are generally synchronous from the Mesoarchean to the Neoarchean. The Mesoarchean depleted mantle-derived mafic magmatism may have provided heat to trigger partial melting of the Eo-to Paleoarchean mafic source for the charnockite-TTG magmatism, and also contributed to their

476 complex geochemical and isotopic compositions. Furthermore, the combined geochemical and
477 whole-rock Sr-Nd-Hf and zircon Hf-O isotopic data suggests that the formation of Mesoarchean
478 continental crust was episodic, with pulses of juvenile mantle-derived mafic material and
479 crustal growth in the Ntem Complex. On the other hand, it has also been proposed that episodic
480 crustal growth could be related to mantle plume activity (e.g. Condie, 1998), but this assumption
481 cannot explain the large volume of arc-like felsic magmatism in the region compared to mafic
482 magmatism. Thus, the formation of the Archean continental crust of the Ntem complex may be
483 related to a combination of Archean accretion and subduction processes.

484 Based on the above, multi-stage magmatism, crustal reworking and growth events occurred
485 in the Ntem Complex at ~3.90 – 3.25 Ga, ~3.25 – 3.00 Ga, ~2.95 – 2.85 Ga and ~2.75 – 2.72
486 Ga from the Eo- to the Neoarchean (Fig. 6).

487 **5.4. Craton scale implications**

488 The Congo Craton is one of the least studied Archean terranes in the world, and is made
489 up of three main blocks: the Kasai Block to the South, the NE Congo and West Nile blocks to
490 the Northeast of D.R. Congo (Bomu Complex), and the Ntem-Chaillu block (Cameroon,
491 Gabon) (Thiéblemont et al., 2018). Available U–Pb zircon ages indicate that the Congo Craton
492 was formed mostly between ca. 3.4 and 2.5 Ga (eg. Cahen et al., 1976; Toteu et al., 1994;
493 Mayaga-Mikolo, 1996; Feybesse et al., 1998; Takam et al., 2009; Maier et al., 2015; Tchameni
494 et al., 2010; Li et al., 2016; Akame et al., 2020a; Turnbull et al., 2021). However, neither
495 spatially resolved Sm–Nd or Lu–Hf isotope studies have been conducted on the Kasai and
496 Bomun terranes. Consequently, the only possible regional comparison within the Congo Craton
497 for the rocks of the Ntem Complex is with those of the Monts de Cristal and Chaillu terranes of
498 Gabon.

In the Monts de Cristal region of northern Gabon, charnockites and TTG gneisses were dated between 3186 and 3120 Ma (Rb/Sr whole-rock ages; Caen-Vachette et al., 1988). However, both U–Pb zircon ages and Nd isotopic data for these rocks are not yet available. Recently, Thiéblemont et al. (2018) reported the compilation of zircon U–Pb ages and Nd isotopic data from Archean granitoid rocks exposed alongside the north Gabon domain and the Chaillu Complex. Zircon extracted from these rocks yielded crystallisation ages from ca. 2.92 Ga to ca. 2.55 Ga with two major magmatic events at ca 2.92 – 2.85 Ga (TTG and charnockites plutonism) and ca 2.8 – 2.6 Ga (Neoarchean magmatic episode), like those of the Ntem Complex. In addition, most of the Mesoarchean felsic rocks show a chondritic to sub-chondritic $\varepsilon^{143}Nd_{(i)}$ signature with $T_{DM}(Nd)$ ages old as 3.2 Ga (de Wit and Linol, 2015b; Thiéblemont et al., 2009, 2018). However, the zircon Hf isotopic composition of the 2.89 Ga TTGs from Ivindo Basement Complex (Republic of Congo) shows positive εHf(t) values of +1.22 to +4.55 and 3.23 – 3.02 Ga $T_{DM}(Hf)$ model ages (Gatsé Ebotehouna et al., 2021), which suggest the existence of a depleted mantle domain underlying the Ivindo Basement Complex. Moreover, these super-chondritic $\varepsilon^{176}Hf$ values differ from the subchondritic values measured in the ca. 2.86 Ga zircon and whole rocks from the Ntem Complex TTG suites (Fig. 5c). We suggest that the NW Congo likely developed from Paleoarchean mafic protoliths that underwent considerable reworking and juvenile accretion additions during the Mesoarchean. Near Mitzic in the Monts de Cristal Complex, meta-kimberlite dykes were emplaced at 2848 − 2862 Ma (zircon U–Pb LA-ICP-MS ; Henning et al., 2003), which suggests a Mesoarchean age for ultramafic–mafic magmatism in the north Gabon domain. These Mesoarchean kimberlite intrusions were synchronous with the dacitic volcanism and mafic magmatism at 2862 − 2883 Ma in the Ntem Complex (Chombong and Suh, 2013; Li et al., 2016; Akame et al., 2020a). The Neoarchean ultramafic–mafic intrusion from the Monts de Cristal Complex (North Gabon terrane) studied by Maier et al. (2015) yielded crystallization ages of ca. 2765 – 2775 Ma with

positive $\varepsilon^{143}Nd_{(i)}$ values (+0.1 to +1.8) and T_{DM}(Nd) ages of 2.96 – 3.06 Ga. While, the Neoarchean anatectic granitoids are sub-chondritic, with $\varepsilon Nd_{(i)}$ values ranging from −1 to −7 (Thiéblemont et al., 2018), indicating the reworking of older felsic crustal rocks. The time for the Bélinga greenstone belt formation (North Gabon domain) is defined between 2918 ± 7 and 2868 ± 9 Ma by U–Pb based on detrital zircons (Thiéblemont et al., 2009, 2018). The ca 2.84 – 2.82 Ga and ~ 2.75 Ga magmatic-metamorphic events in the north Gabon domain (Thiéblemont et al., 2009, 2011, 2018) have also been reported in the Sangmelima area (Akame et al., 2020a, 2021). Overall, according to the current geochronological and isotopic data, it is evident that the entire Ntem-Chaillu block or NW Congo Craton experienced the same geodynamic evolution.

From above, we conclude that minor Paleoarchean crust existed in the NW Congo Craton with the generation started at ~ 3.5 Ga likely by melting of mafic crust extracted from the mantle at ~ 3.8 −3.3 Ga (Fig. 6). Finally, all the NW Congo craton Archean underwent important episodes of crustal generation and reworking from the Mesoarchean to Neoarchean.

6. Conclusions

We present the first coupled whole-rock ^{176}Lu–^{176}Hf and ^{147}Sm–^{143}Nd dataset for Archean felsic and mafic rocks from the NW Congo Craton. Sixteen mafic and felsic igneous rocks were collected in the Sangmelima terranes, located in the northern part of the Ntem Complex, southern Cameroon. The mafic rocks include 2.87 Ga gabbronorites and late 2.72 Ga dolerite dykes. The granitoids include 2.91 Ga charnockites, 2.87 Ga TTG suites, and 2.75 Ga high-K granites. Some isotopic data suggest post-crystallisation modification of the whole-rock Sm−Nd isotopic system during the Mesoarchean tectonothermal events. All the Mesoarchean charnockite and TTG samples we analysed show negative $\varepsilon^{176}Hf_{(i)}$ = – 0.9 to –7.4 and $\varepsilon^{143}Nd_{(i)}$ = –1.9 to –5.1 with average Hf and Nd depleted mantle model ages of ~ 3.30 Ga and 3.37 Ga, respectively. The Hf-Nd isotopic composition ($\varepsilon^{176}Hf_{(i)}$ = –3.7 and $\varepsilon^{143}Nd_{(i)}$ = –4.6) of high-K granite (2.75 Ga) is consistent with derivation by re-melting of an enriched crustal source at ~

3.2 Ga. The depleted $\varepsilon^{176}Hf_{(i)}$ and $\varepsilon^{143}Nd_{(i)}$ values (+3.4 to +8.2 and +0.9 to +1.6, respectively) in the Sangmelima Mesoarchean gabbronorites highlight a depleted mantle source. The whole set of the geochronological and isotopic data in the Ntem Complex and other domains of NW Congo Craton like Monts de Cristal and Chaillu Complex in Gabon and the Ivindo Basement Complex (Republic of Congo) revealed that minor Paleoarchean crust existed in the NW Congo Craton with the generation starting at ~ 3.5 Ga likely by melting of mafic crust extracted from the mantle at ~ 3.8 − 3.3 Ga. Subsequently, all Archean basement domains underwent considerable reworking and juvenile accretion additions during the Mesoarchean. Collectively, the Archean crustal accretion is characterised by multi-stage magmatism, crustal reworking, and growth events that occurred at ~3.90 – 3.30 Ga, ~3.25 – 3.0 Ga, ~2.95 – 2.85 Ga and ~2.75 – 2.72 Ga in the NW Congo.

Acknowledgements

We are grateful to Sabrina Cauchies for trace element measurements and isotope purification, and to Jeroen de Jong for Nd and Hf isotopes measurements on the Nu-Plasma II at ULB.

We also want to acknowledge Prof. Tony Kemp for his editorial handling, Dr. Jonas Tusch and an anonymous reviewer for their positive and constructive comments which greatly helped to improve the final version of the manuscript. We also thank Dr. Fabien Humbert for her help and constructive suggestions. JMA thanks the grant "Prix de Meurs-Francois", ULB, Fédération Wallonie-Bruxelles, and *MOPGA 2022 Visiting Fellowship Program for Young Researchers* for current support. VD thanks the EoS project ET-Home and FRS-FNRS for support.

References

Akame, J.M., Oliveira, E.P., Poujol, M., Hublet, G., Debaille, V., 2020a. LA–ICP–MS zircon U Pb dating, Lu Hf, Sm Nd geochronology and tectonic setting of the Mesoarchean mafic and felsic magmatic rocks in the Sangmelima granite-greenstone terrane, Ntem Complex (South Cameroon). Lithos 372–373, 105702. https://doi.org/10.1016/j.lithos.2020.105702

577 Akame, J.M., Owona, S., Hublet, G., Debaille, V., 2020b. Archean tectonics in the sangmelima
578 granite-greenstone terrains, Ntem Complex (NW Congo craton), southern Cameroon. Journal
579 of African Earth Sciences 168, 103872. https://doi.org/10.1016/j.jafrearsci.2020.103872
580 Akame, J.M., Schulz, B., Owona, S., Debaille, V., 2021. Monazite EPMA-CHIME dating of
581 Sangmelima granulite and granitoid rocks in the Ntem Complex, Cameroon: Implications for
582 Archean tectono-thermal evolution of NW Congo craton. Journal of African Earth Sciences
583 181, 104268. https://doi.org/10.1016/j.jafrearsci.2021.104268
584 Amelin, Y., Lee, D.-C., Halliday, A.N., Pidgeon, R.T., 1999. Nature of the Earth's earliest crust from
585 hafnium isotopes in single detrital zircons. Nature 399, 252–255.
586 https://doi.org/10.1038/20426
587 Anders, E., Grevesse, N., 1989. Abundances of the elements: Meteoritic and solar. Geochimica et
588 Cosmochimica Acta 53, 197–214. https://doi.org/10.1016/0016-7037(89)90286-X
589 Bea, F., Montero, P., Molina, J.F., Scarrow, J.H., Cambeses, A., Moreno, J.A., 2018. Lu-Hf ratios of
590 crustal rocks and their bearing on zircon Hf isotope model ages: The effects of accessories.
591 Chemical Geology 484, 179–190. https://doi.org/10.1016/j.chemgeo.2017.11.034
592 Blichert-Toft, J., 2001. On the Lu-Hf Isotope Geochemistry of Silicate Rocks. Geostandards and
593 Geoanalytical Research 25, 41–56. https://doi.org/10.1111/j.1751-908X.2001.tb00786.x
594 Blichert-Toft, J., Puchtel, I.S., 2010. Depleted mantle sources through time: Evidence from Lu–Hf and
595 Sm–Nd isotope systematics of Archean komatiites. Earth and Planetary Science Letters 297,
596 598–606. https://doi.org/10.1016/j.epsl.2010.07.012
597 Bodet, F., Schärer, U., 2000. Evolution of the SE-Asian continent from U-Pb and Hf isotopes in single
598 grains of zircon and baddeleyite from large rivers. Geochimica et Cosmochimica Acta 64,
599 2067–2091. https://doi.org/10.1016/S0016-7037(00)00352-5
600 Bouvier, A., Vervoort, J.D., Patchett, P.J., 2008. The Lu–Hf and Sm–Nd isotopic composition of
601 CHUR: Constraints from unequilibrated chondrites and implications for the bulk composition
602 of terrestrial planets. Earth and Planetary Science Letters 273, 48–57.
603 https://doi.org/10.1016/j.epsl.2008.06.010
604 Caen-Vachette, M., Vialette, Y., Bassot, J.P., Vidal, P., 1988. Apport de la géochronologie isotopique
605 à la connaissance de la géologie gabonaise. Chron. rech. min 491, 35–53.
606 Cahen, L., Delhal, J., Lavreau, J., 1976. The archaean of equatorial Africa: a review. The Early
607 History of the Earth. Wiley, New York 486–498.
608 Caro, G., Bourdon, B., Wood, B.J., Corgne, A., 2005. Trace-element fractionation in Hadean mantle
609 generated by melt segregation from a magma ocean. Nature 436, 246–249.
610 https://doi.org/10.1038/nature03827
611 Cawood, P.A., Hawkesworth, C.J., Pisarevsky, S.A., Dhuime, B., Capitanio, F.A., Nebel, O., 2018.
612 Geological archive of the onset of plate tectonics. Phil. Trans. R. Soc. A. 376, 20170405.
613 https://doi.org/10.1098/rsta.2017.0405
614 Chauvel, C., Blichert-Toft, J., 2001. A hafnium isotope and trace element perspective on melting of
615 the depleted mantle. Earth and Planetary Science Letters 190, 137–151.
616 https://doi.org/10.1016/S0012-821X(01)00379-X
617 Chombong, N.N., Suh, C.E., 2013. 2883 Ma commencement of BIF deposition at the northern edge of
618 Congo craton, southern Cameroon: new zircon SHRIMP data constraint from metavolcanics.
619 Episodes 36, 47–57.
620 Condie, K.C., 1998. Episodic continental growth and supercontinents: a mantle avalanche connection?
621 Earth and Planetary Science Letters 163, 97–108.
622 Condie, K.C., 1994. Archean crustal evolution. Elsevier.
623 Condie, K.C., 1986. Origin and early growth rate of continents. Precambrian Research 32, 261–278.
624 https://doi.org/10.1016/0301-9268(86)90032-X
625 de Wit, M.J., Ashwal, L.D., 1995. Greenstone belts: what are they? South African Journal of Geology
626 98, 505–520.
627 de Wit, M.J., Linol, B., 2015a. Precambrian Basement of the Congo Basin and Its Flanking Terrains,
628 in: de Wit, M.J., Guillocheau, F., de Wit, M.C.J. (Eds.), Geology and Resource Potential of
629 the Congo Basin. Springer Berlin Heidelberg, Berlin, Heidelberg, pp. 19–37.
630 https://doi.org/10.1007/978-3-642-29482-2_2

de Wit, M.J., Linol, B., 2015b. Precambrian Basement of the Congo Basin and Its Flanking Terrains, in: de Wit, M.J., Guillocheau, F., de Wit, M.C.J. (Eds.), Geology and Resource Potential of the Congo Basin. Springer Berlin Heidelberg, Berlin, Heidelberg, pp. 19–37. https://doi.org/10.1007/978-3-642-29482-2_2

Debaille, V., Brandon, A.D., Yin, Q.Z., Jacobsen, B., 2007. Coupled 142Nd–143Nd evidence for a protracted magma ocean in Mars. Nature 450, 525–528. https://doi.org/10.1038/nature06317

Debaille, V., O'Neill, C., Brandon, A.D., Haenecour, P., Yin, Q.-Z., Mattielli, N., Treiman, A.H., 2013. Stagnant-lid tectonics in early Earth revealed by 142Nd variations in late Archean rocks. Earth and Planetary Science Letters 373, 83–92. https://doi.org/10.1016/j.epsl.2013.04.016

DePaolo, D.J., 1981. Neodymium isotopes in the Colorado Front Range and crust–mantle evolution in the Proterozoic. Nature 291, 193–196. https://doi.org/10.1038/291193a0

Feybesse, J.L., Johan, V., Triboulet, C., Guerrot, C., Mayaga-Mikolo, F., Bouchot, V., N'dong, J.E., 1998. The West Central African belt: a model of 2.5–2.0 Ga accretion and two-phase orogenic evolution. Precambrian Research 87, 161–216.

Fisher, C.M., Bauer, A.M., Vervoort, J.D., 2020. Disturbances in the Sm–Nd isotope system of the Acasta Gneiss Complex—Implications for the Nd isotope record of the early Earth. Earth and Planetary Science Letters 530, 115900. https://doi.org/10.1016/j.epsl.2019.115900

Furnes, H., Dilek, Y., de Wit, M., 2015. Precambrian greenstone sequences represent different ophiolite types. Gondwana Research 27, 649–685. https://doi.org/10.1016/j.gr.2013.06.004

Gatsé Ebotehouna, C., Xie, Y., Adomako- Ansah, K., Qu, Y., 2021. Petrology, geochemistry, and zircon U–Pb- Lu–Hf isotopes of granitoids from the Ivindo Basement Complex of the Souanké Area, Republic of Congo: Insights into the evolution of Archean continental crust. Geological Journal 56, 4861–4887. https://doi.org/10.1002/gj.4219

Goldstein, S.L., O'Nions, R.K., Hamilton, P.J., 1984. A Sm-Nd isotopic study of atmospheric dusts and particulates from major river systems. Earth and Planetary Science Letters 70, 221–236. https://doi.org/10.1016/0012-821X(84)90007-4

Goodwin, A.M., 1981. Chapter 5 Archaean Plates and Greenstone Belts, in: Developments in Precambrian Geology. Elsevier, pp. 105–135. https://doi.org/10.1016/S0166-2635(08)70010-0

Griffin, W.L., Wang, X., Jackson, S.E., Pearson, N.J., O'Reilly, S.Y., Xu, X., Zhou, X., 2002. Zircon chemistry and magma mixing, SE China: In-situ analysis of Hf isotopes, Tonglu and Pingtan igneous complexes. Lithos 61, 237–269. https://doi.org/10.1016/S0024-4937(02)00082-8

Halla, J., Whitehouse, M.J., Ahmad, T., Bagai, Z., 2017. Archaean granitoids: an overview and significance from a tectonic perspective. Geological Society, London, Special Publications 449, 1–18.

Hammerli, J., Kemp, A.I.S., 2021. Combined Hf and Nd isotope microanalysis of co-existing zircon and REE-rich accessory minerals: High resolution insights into crustal processes. Chemical Geology 581, 120393. https://doi.org/10.1016/j.chemgeo.2021.120393

Hammerli, J., Kemp, A.I.S., Spandler, C., 2014. Neodymium isotope equilibration during crustal metamorphism revealed by in situ microanalysis of REE-rich accessory minerals. Earth and Planetary Science Letters 392, 133–142. https://doi.org/10.1016/j.epsl.2014.02.018

Hammerli, J., Kemp, A.I.S., Whitehouse, M.J., 2019. In situ trace element and Sm-Nd isotope analysis of accessory minerals in an Eoarchean tonalitic gneiss from Greenland: Implications for Hf and Nd isotope decoupling in Earth's ancient rocks. Chemical Geology 524, 394–405. https://doi.org/10.1016/j.chemgeo.2019.06.025

Hasenstab, E., Tusch, J., Schnabel, C., Marien, C.S., Van Kranendonk, M.J., Smithies, H., Howard, H., Maier, W.D., Münker, C., 2021. Evolution of the early to late Archean mantle from Hf-Nd-Ce isotope systematics in basalts and komatiites from the Pilbara Craton. Earth and Planetary Science Letters 553, 116627. https://doi.org/10.1016/j.epsl.2020.116627

Henning, A., Kiviets, G., Kurszlaukis, S., Barton, E., Mayaga-Mikolo, F., 2003. Early Proterozoic metamorphosed kimberlites from Gabon, in: International Kimberlite Conference: Extended Abstracts.

Hoffmann, J.E., Nagel, T.J., Münker, C., Næraa, T., Rosing, M.T., 2014. Constraining the process of Eoarchean TTG formation in the Itsaq Gneiss Complex, southern West Greenland. Earth and Planetary Science Letters 388, 374–386. https://doi.org/10.1016/j.epsl.2013.11.050

685 Iizuka, T., Hirata, T., Komiya, T., Rino, S., Katayama, I., Motoki, A., Maruyama, S., 2005. U-Pb and
686 Lu-Hf isotope systematics of zircons from the Mississippi River sand: Implications for
687 reworking and growth of continental crust. Geol 33, 485. https://doi.org/10.1130/G21427.1
688 Kemp, A.I.S., Hawkesworth, C.J., Foster, G.L., Paterson, B.A., Woodhead, J.D., Hergt, J.M., Gray,
689 C.M., Whitehouse, M.J., 2007. Magmatic and Crustal Differentiation History of Granitic
690 Rocks from Hf-O Isotopes in Zircon. Science 315, 980–983.
691 https://doi.org/10.1126/science.1136154
692 Laurent, O., Martin, H., Moyen, J.F., Doucelance, R., 2014. The diversity and evolution of late-
693 Archean granitoids: Evidence for the onset of "modern-style" plate tectonics between 3.0 and
694 2.5Ga. Lithos 205, 208–235. https://doi.org/10.1016/j.lithos.2014.06.012
695 Li, X.H., Chen, Y., Li, J., Yang, C., Ling, X.-X., Tchouankoue, J.P., 2016. New isotopic constraints on
696 age and origin of Mesoarchean charnockite, trondhjemite and amphibolite in the Ntem
697 Complex of NW Congo Craton, southern Cameroon. Precambrian Research 276, 14–23.
698 https://doi.org/10.1016/j.precamres.2016.01.027
699 Ludwig, K.R., 2012. Berkeley Geochronology Center Special Publication No. 5 75.
700 Maier, W.D., Rasmussen, B., Fletcher, I.R., Godel, B., Barnes, S.J., Fisher, L.A., Yang, S.H., Huhma,
701 H., Lahaye, Y., 2015. Petrogenesis of the ~2·77 Ga Monts de Cristal Complex, Gabon:
702 Evidence for Direct Precipitation of Pt-arsenides from Basaltic Magma. J. Petrology 56, 1285–
703 1308. https://doi.org/10.1093/petrology/egv035
704 Martin, H., 1987. Petrogenesis of Archaean Trondhjemites, Tonalites, and Granodiorites from Eastern
705 Finland: Major and Trace Element Geochemistry. Journal of Petrology 28, 921–953.
706 https://doi.org/10.1093/petrology/28.5.921
707 Martin, H., 1986. Effect of steeper Archean geothermal gradient on geochemistry of subduction-zone
708 magmas. Geology 14, 753–756.
709 Martin, H., Moyen, J.-F., Guitreau, M., Blichert-Toft, J., Le Pennec, J.-L., 2014. Why Archaean TTG
710 cannot be generated by MORB melting in subduction zones. Lithos 198–199, 1–13.
711 https://doi.org/10.1016/j.lithos.2014.02.017
712 Maurizot, P., Abessolo, A., Feybesse, J.L., Johan, L.P., 1986. Etude et prospection minière du Sud-
713 Ouest Cameroun, synthèse des travaux de 1978 a 1985. Rapport du BRGM№ 85.
714 Mayaga-Mikolo, F., 1996. Chronologie des evenements sedimentaires, magmatiques et tectono-
715 metamorphiques du precambrien d'afrique centrale occidentale (gabon): tectogenese ogooue
716 et heritage archeen (PhD Thesis). Clermont-Ferrand 2.
717 McCulloch, M.T., Bennett, V.C., 1994. Progressive growth of the Earth's continental crust and
718 depleted mantle: Geochemical constraints. Geochimica et Cosmochimica Acta 58, 4717–4738.
719 https://doi.org/10.1016/0016-7037(94)90203-8
720 Moyen, J.-F., 2011. The composite Archaean grey gneisses: Petrological significance, and evidence
721 for a non-unique tectonic setting for Archaean crustal growth. Lithos 123, 21–36.
722 https://doi.org/10.1016/j.lithos.2010.09.015
723 Moyen, J.-F., Martin, H., 2012. Forty years of TTG research. Lithos 148, 312–336.
724 https://doi.org/10.1016/j.lithos.2012.06.010
725 Nebel, O., Campbell, I.H., Sossi, P.A., Van Kranendonk, M.J., 2014. Hafnium and iron isotopes in
726 early Archean komatiites record a plume-driven convection cycle in the Hadean Earth. Earth
727 and Planetary Science Letters 397, 111–120. https://doi.org/10.1016/j.epsl.2014.04.028
728 Patiño Douce, A.E., Beard, J.S., 1995. Dehydration-melting of Biotite Gneiss and Quartz Amphibolite
729 from 3 to 15 kbar. J Petrology 36, 707–738. https://doi.org/10.1093/petrology/36.3.707
730 Polat, A., Hofmann, A.W., 2003. Alteration and geochemical patterns in the 3.7–3.8 Ga Isua
731 greenstone belt, West Greenland. Precambrian Research 126, 197–218.
732 https://doi.org/10.1016/S0301-9268(03)00095-0
733 Pouclet, A., Tchameni, R., Mezger, K., Vidal, M., Nsifa, E., Shang, C., Penaye, J., 2007. Archaean
734 crustal accretion at the northern border of the Congo Craton (South Cameroon). The
735 charnockite-TTG link. Bulletin de la Societe Geologique de France 178, 331–342.
736 https://doi.org/10.2113/gssgfbull.178.5.331
737 Rizo, H., Boyet, M., Blichert-Toft, J., Rosing, M., 2011. Combined Nd and Hf isotope evidence for
738 deep-seated source of Isua lavas. Earth and Planetary Science Letters 312, 267–279.
739 https://doi.org/10.1016/j.epsl.2011.10.014

740 Roth, E., Bank, T.L., Granite, E., 2018. Investigation of Thulium and Other Rare Earth Element Mass
741 Fractions in NIST SRM 1632a Bituminous Coal Reference Material by Quadrupole ICP-MS.
742 Geostand Geoanal Res 42, 263–269. https://doi.org/10.1111/ggr.12203
743 Salerno, R., Vervoort, J., Fisher, C., Kemp, A., Roberts, N., 2021. The coupled Hf-Nd isotope record
744 of the early Earth in the Pilbara Craton. Earth and Planetary Science Letters 572, 117139.
745 https://doi.org/10.1016/j.epsl.2021.117139
746 Shafer, J.T., Brandon, A.D., Lapen, T.J., Righter, M., Peslier, A.H., Beard, B.L., 2010. Trace element
747 systematics and 147Sm–143Nd and 176Lu–176Hf ages of Larkman Nunatak 06319: Closed-
748 system fractional crystallization of an enriched shergottite magma. Geochimica et
749 Cosmochimica Acta 74, 7307–7328. https://doi.org/10.1016/j.gca.2010.09.009
750 Shang, C.K., Liégeois, J.P., Satir, M., Frisch, W., Nsifa, E.N., 2010. Late Archaean high-K granite
751 geochronology of the northern metacratonic margin of the Archaean Congo craton, Southern
752 Cameroon: Evidence for Pb-loss due to non-metamorphic causes. Gondwana Research 18,
753 337–355. https://doi.org/10.1016/j.gr.2010.02.008
754 Shang, C.K., Satir, M., Nsifa, E.N., Liégeois, J.-P., Siebel, W., Taubald, H., 2007. Archaean high-K
755 granitoids produced by remelting of earlier Tonalite–Trondhjemite–Granodiorite (TTG) in the
756 Sangmelima region of the Ntem complex of the Congo craton, southern Cameroon. Int J Earth
757 Sci (Geol Rundsch) 96, 817–841. https://doi.org/10.1007/s00531-006-0141-3
758 Shang, C.K., Satir, M., Siebel, W., Nsifa, E.N., Taubald, H., Liégeois, J.P., Tchoua, F.M., 2004a. TTG
759 magmatism in the Congo craton; a view from major and trace element geochemistry, Rb–Sr
760 and Sm–Nd systematics: case of the Sangmelima region, Ntem complex, southern Cameroon.
761 Journal of African Earth Sciences 40, 61–79. https://doi.org/10.1016/j.jafrearsci.2004.07.005
762 Shang, Siebel, W., Satir, M., Chen, F., Mvondo, J.O., 2004b. Zircon Pb-Pb and U-Pb systematics of
763 TTG rocks in the Congo Craton: Constraints on crust formation, magmatism, and Pan-African
764 lead loss. Bulletin of Geosciences 79, 205–219.
765 Smithies, R.H., 2000. The Archaean tonalite–trondhjemite–granodiorite (TTG) series is not an
766 analogue of Cenozoic adakite. Earth and Planetary Science Letters 182, 115–125.
767 https://doi.org/10.1016/S0012-821X(00)00236-3
768 Smithies, R.H., Ivanic, T.J., Lowrey, J.R., Morris, P.A., Barnes, S.J., Wyche, S., Lu, Y.-J., 2018. Two
769 distinct origins for Archean greenstone belts. Earth and Planetary Science Letters 487, 106–
770 116. https://doi.org/10.1016/j.epsl.2018.01.034
771 Sproule, R.A., Lesher, C.M., Ayer, J.A., Thurston, P.C., Herzberg, C.T., 2002. Spatial and temporal
772 variations in the geochemistry of komatiites and komatiitic basalts in the Abitibi greenstone
773 belt. Precambrian Research 115, 153–186. https://doi.org/10.1016/S0301-9268(02)00009-8
774 Sun, S. -s., McDonough, W.F., 1989. Chemical and isotopic systematics of oceanic basalts:
775 implications for mantle composition and processes. Geological Society, London, Special
776 Publications 42, 313–345. https://doi.org/10.1144/GSL.SP.1989.042.01.19
777 Takam, T., Arima, M., Kokonyangi, J., Dunkley, D.J., Nsifa, E.N., 2009. Paleoarchaean charnockite in
778 the Ntem Complex, Congo Craton, Cameroon: insights from SHRIMP zircon U-Pb ages.
779 Journal of Mineralogical and Petrological Sciences 104, 1–11.
780 https://doi.org/10.2465/jmps.080624
781 Tchameni, R., Lerouge, C., Penaye, J., Cocherie, A., Milesi, J.P., Toteu, S.F., Nsifa, N.E., 2010.
782 Mineralogical constraint for metamorphic conditions in a shear zone affecting the Archean
783 Ngoulemakong tonalite, Congo craton (Southern Cameroon) and retentivity of U–Pb SHRIMP
784 zircon dates. Journal of African Earth Sciences 58, 67–80.
785 https://doi.org/10.1016/j.jafrearsci.2010.01.009
786 Tchameni, R., Mezger, K., Nsifa, N.E., Pouclet, A., 2000. Neoarchæan crustal evolution in the Congo
787 Craton: evidence from K rich granitoids of the Ntem Complex, southern Cameroon. Journal of
788 African Earth Sciences 30, 133–147. https://doi.org/10.1016/S0899-5362(00)00012-9
789 Tchameni, R., Pouclet, A., Mezger, K., Nsifa, N.E., Vicat, J.P., 2004. Single zircon Pb-Pb and Sm-Nd
790 whole rock ages for the Ebolowa greenstone belts: Evidence for pre-2.9 Ga terranes in the
791 Ntem Complex (South Cameroon). Journal of the Cameroon Academy of Sciences 4, 235–
792 246.
793 Thiéblemont, D., Agenbacht, A., Boulingui, B.B., Bouton, P., Ekhoga, H., Goujou, J.-C., Kassadou,
794 A.B., Moussavou, M., Prian, J.-P., Theunissen, K., 2011. Synchronous BIF, HT

metamorphism and granitic plutonism at ca. 2.8 Ga in Gabon, in: 23th Congress on African Geology.
Thiéblemont, D., Callec, Y., Fernandez-Alonso, M., Chène, F., 2018. A Geological and Isotopic Framework of Precambrian Terrains in Western Central Africa: An Introduction, in: Siegesmund, S., Basei, M.A.S., Oyhantçabal, P., Oriolo, S. (Eds.), Geology of Southwest Gondwana. Springer International Publishing, Cham, pp. 107–132. https://doi.org/10.1007/978-3-319-68920-3_5
Thiéblemont, D., Castaing, C., Billa, M., Bouton, P., Préat, A., 2009. Notice explicative de la carte géologique et des ressources minérales de la République Gabonaise à 1/1000000. Programme Sysmin 8, 384.
Toteu, S.F., Van Schmus, W.R., Penaye, J., Nyobé, J.B., 1994. U□Pb and Sm□N edvidence for Eburnian and Pan-African high-grade metamorphism in cratonic rocks of southern Cameroon. Precambrian Research 67, 321–347. https://doi.org/10.1016/0301-9268(94)90014-0
Turnbull, R.E., Allibone, A.H., Matheys, F., Fanning, C.M., Kasereka, E., Kabete, J., McNaughton, N.J., Mwandale, E., Holliday, J., 2021. Geology and geochronology of the Archean plutonic rocks in the northeast Democratic Republic of Congo. Precambrian Research 358, 106133. https://doi.org/10.1016/j.precamres.2021.106133
Vervoort, J., 2014. Evolution of the depleted mantle and growth of the continental crust: An early beginning or a slow start? 14683.
Vervoort, J.D., Blichert-Toft, J., 1999. Evolution of the depleted mantle: Hf isotope evidence from juvenile rocks through time. Geochimica et Cosmochimica Acta 63, 533–556. https://doi.org/10.1016/S0016-7037(98)00274-9
Vervoort, J.D., Plank, T., Prytulak, J., 2011. The Hf–Nd isotopic composition of marine sediments. Geochimica et Cosmochimica Acta 75, 5903–5926. https://doi.org/10.1016/j.gca.2011.07.046
Vicat, J.-P., LEGER, J.-M., NSIFA, E., PIGUET, P., NZENTI, J.-P., TCHAMENI, R., POUCLET, A., 1996. Distinction, au sein du craton congolais du Sud-Ouest du Cameroun, de deux épisodes doléritiques initiant les cycles orogéniques éburnéen (Paléoprotérozoïque) et panafricain (Néoprotérozoïque). C. r. Acad. sci., Sér. 2, Sci. terre planet 323, 575–582.
Viehmann, S., Bau, M., Hoffmann, J.E., Münker, C., 2018. Decoupled Hf and Nd isotopes in suspended particles and in the dissolved load of Late Archean seawater. Chemical Geology 483, 111–118. https://doi.org/10.1016/j.chemgeo.2018.01.017
Wainwright, A.N., El Atrassi, F., Debaille, V., Mattielli, N., 2019. Geochemistry and petrogenesis of Archean mafic rocks from the Amsaga area, West African craton, Mauritania. Precambrian Research 324, 208–219. https://doi.org/10.1016/j.precamres.2019.02.005
Watkins, J.M., Clemens, J.D., Treloar, P.J., 2007. Archaean TTGs as sources of younger granitic magmas: melting of sodic metatonalites at 0.6–1.2 GPa. Contrib Mineral Petrol 154, 91–110. https://doi.org/10.1007/s00410-007-0181-0
Weis, D., Kieffer, B., Hanano, D., Nobre Silva, I., Barling, J., Pretorius, W., Maerschalk, C., Mattielli, N., 2007. Hf isotope compositions of U.S. Geological Survey reference materials: USGS REFERENCE MATERIALS. Geochem. Geophys. Geosyst. 8, n/a-n/a. https://doi.org/10.1029/2006GC001473

Figure captions

Figure 1. a) Regional geological map of the Ntem Complex, and thrust contact with the Pan-African fold belt in Southern Cameroon modified after Maurizot et al. (1986). b) Simplified geological map of the Sangmelima region and sample locations.

Figure 2. (a-c) N-MORB and primitive-mantle normalised trace-element patterns and (b-d) chondrite-normalised REE patterns for the mafic rocks and granitoids. The trace elemental data are from Akame et al. (2020a). Primitive mantle and NMORB values are from Sun and McDonough, (1989) and chondrite values are from Anders and Grevesse (1989)

Figure 3. Lu-Hf and Sm-Nd isochron diagrams for Sangmelima igneous rocks.

Figure 4. a) $\varepsilon Hf_{(i)}$ *vs.* $\varepsilon Nd_{(i)}$ from Sangmelima igneous rocks. Two mafic samples (AJM16 and AJM17) are decoupled in their $\varepsilon Hf_{(i)}$ and $\varepsilon Nd_{(i)}$ composition, which can be explained by crustal contamination or secondary alteration due to metamorphism. b) Binary diagrams of Zr versus selected elements for the whole-rock samples.

Figure 5. (a) Measured $^{176}Hf/^{177}Hf$ vs. 1/Hf and (b) measured $^{143}Nd/^{144}Nd$ vs. 1/Nd. (c) $\varepsilon Hf_{(i)}$ vs. age (Ma) and (d) $\varepsilon Nd_{(i)}$ vs. age (Ma) diagrams for the igneous rocks.

Figure 6. A timeline of Ntem Complex crustal evolution processes during Archean. Zircon U-Pb dates are provided by Toteu et al. (1994), Takam et al. (2009), Tchameni et al. (2010), Chombong and Suh (2013), Li et al. (2016) and Akame et al., 2020a). Zircon Pb-Pb evaporation ages from Pouclet et al. (2007), Shang et al. (2004b, 2007, 2010). EPMA monazite U-Th- Pb ages from Akame et al. (2021). The probability density curve of the model ages is obtained by combining the bulk-rock Nd model ages (Tchameni et al., 2004; re-calculated Shang et al., 2004a, 2010; re-calculated from Pouclet et al., 2007) and the whole rock Nd-Hf model ages calculated in this study. Zircon Hf model ages are from Li et al. (2016)

Tables.

Table 1.

Major (wt%) and trace (ppm) element contents of Sangmelima igneous rocks

Table 2.

Bulk-rock Sm–Nd and Lu–Hf isotope data for granitoids and mafic rocks of Sangmelima area

Declaration of interests

☒ The authors declare that they have no known competing financial interests or personal relationships that could have appeared to influence the work reported in this paper.

☐The authors declare the following financial interests/personal relationships which may be considered as potential competing interests:

Joseph Martial AKAME[1]*, Vinciane DEBAILLE[1], Marc POUJOL[2],
Corresponding author: Joseph Martial. AKAME: Now at Geosciences Rennes UMR CNRS 6118, Université Rennes 1, 35042 Rennes cedex, France
Email: akamejosephmartial@gmail.com; joseph-martial.akame@univ-rennes1.fr

[1]Laboratoire G-Time Département Géosciences, Environnement, Société
CP 160/02 Avenue F.D. Roosevelt, 50 B-1050 Bruxelles , Belgium
[2]Geosciences Rennes UMR CNRS 6118, Université Rennes 1, 35042 Rennes cedex, France

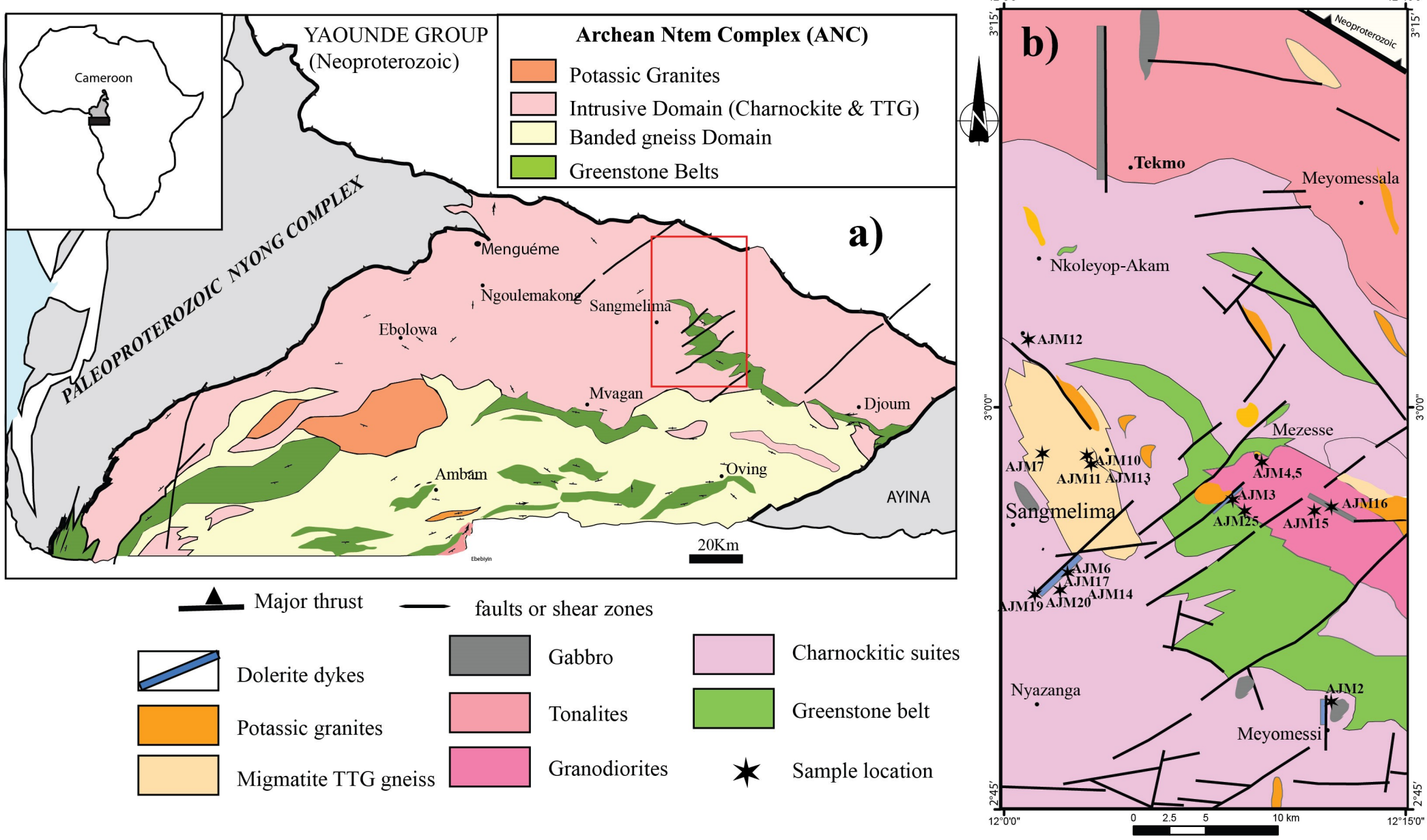
Cameroon
YAOUNDE GROUP
(Neoproterozoic)
Archean Ntem Complex (ANC)
Potassic Granites
Intrusive Domain (Charnockite & TTG)
Banded gneiss Domain
Greenstone Belts
PALEOPROTEROZOIC NYONG COMPLEX
a)
Menguéme
Ngoulemakong
Sangmelima
Ebolowa
Mvagan
Djoum
Ambam
Oving
AYINA
20Km
Ebebiyin
Major thrust
faults or shear zones
Dolerite dykes
Potassic granites
Migmatite TTG gneiss
Gabbro
Tonalites
Granodiorites
Charnockitic suites
Greenstone belt
Sample location
b)
Neoproterozoic
Tekmo
Meyomessala
Nkoleyop-Akam
AJM12
Mezesse
AJM7
AJM10
AJM11
AJM13
AJM4,5
AJM3
AJM16
Sangmelima
AJM25
AJM15
AJM6
AJM17
AJM14
AJM19
AJM20
Nyazanga
AJM2
Meyomessi
12°0'0"
12°15'0"
3°15'
3°0'0"
2°45'
0
2.5
5
10 km

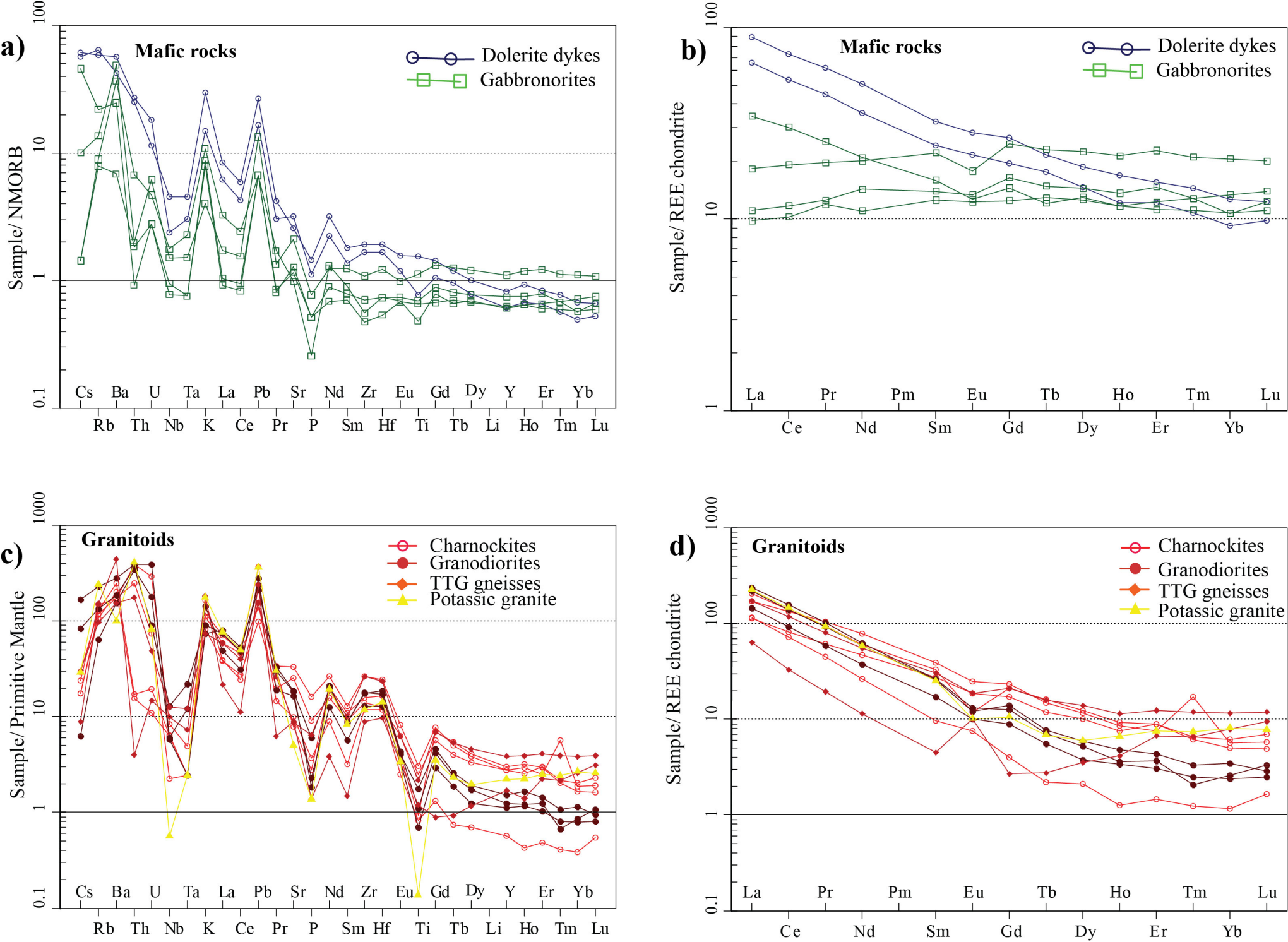
a)
Mafic rocks
Dolerite dykes
Gabbronorites
Sample/ NMORB
100
10
1
0.1
Cs Ba U Ta La Pb Sr Nd Zr Eu Gd Dy Y Er Yb
Rb Th Nb K Ce Pr P Sm Hf Ti Tb Li Ho Tm Lu
b)
Mafic rocks
Dolerite dykes
Gabbronorites
Sample/ REE chondrite
100
10
1
La Pr Pm Eu Tb Ho Tm Lu
Ce Nd Sm Gd Dy Er Yb
c)
Granitoids
Charnockites
Granodiorites
TTG gneisses
Potassic granite
Sample/ Primitive Mantle
1000
100
10
1
0.1
Cs Ba U Ta La Pb Sr Nd Zr Eu Gd Dy Y Er Yb
Rb Th Nb K Ce Pr P Sm Hf Ti Tb Li Ho Tm Lu
d)
Granitoids
Charnockites
Granodiorites
TTG gneisses
Potassic granite
Sample/ REE chondrite
1000
100
10
1
0.1
La Pr Pm Eu Tb Ho Tm Lu
Ce Nd Sm Gd Dy Er Yb

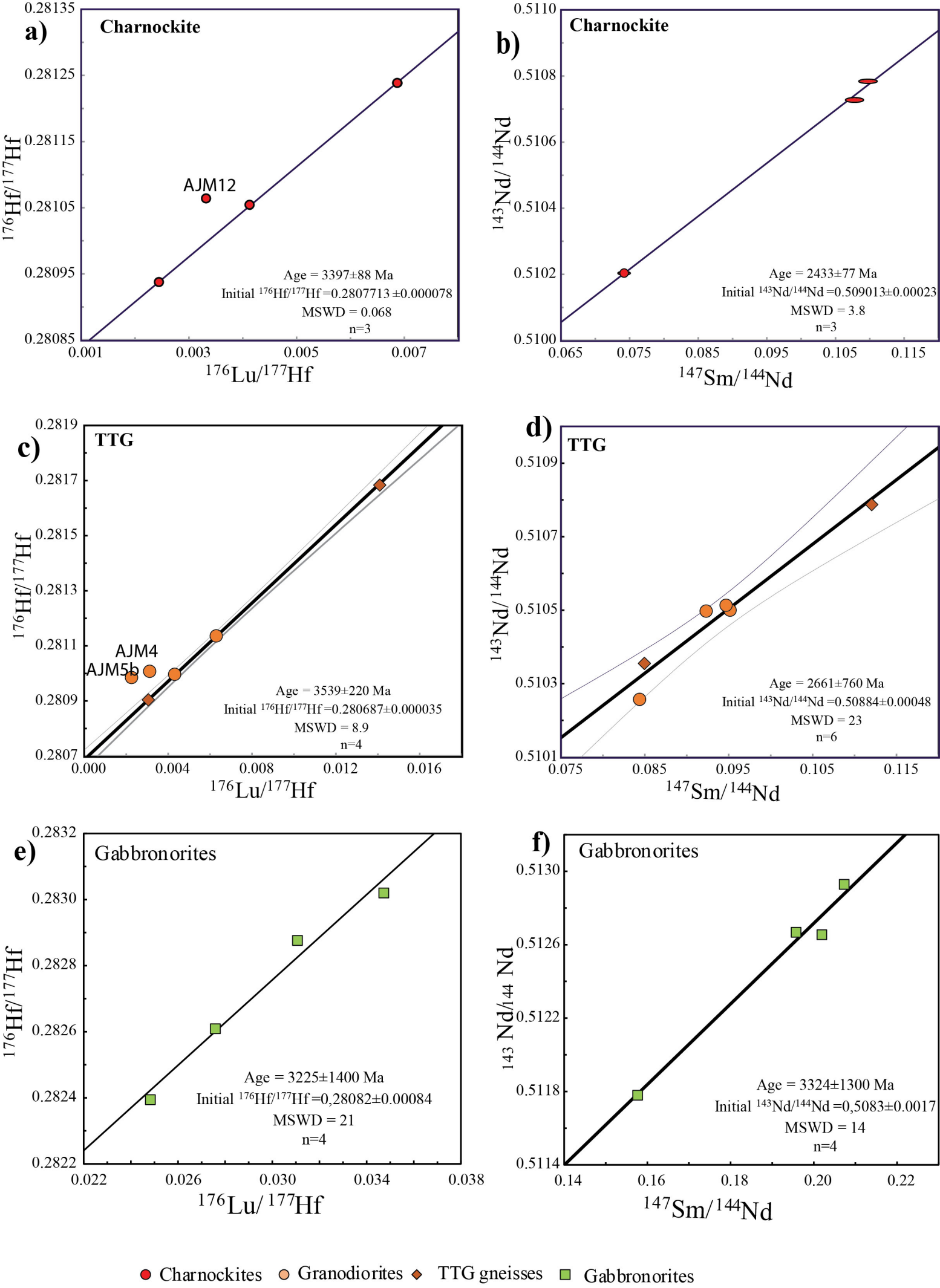
a)
Charnockite
AJM12
Age = 3397±88 Ma
Initial 176Hf/177Hf =0.2807713 ±0.000078
MSWD = 0.068
n=3
176Hf/177Hf
176Lu/177Hf
b)
Charnockite
Age = 2433±77 Ma
Initial 143Nd/144Nd =0.509013±0.00023
MSWD = 3.8
n=3
143Nd/144Nd
147Sm/144Nd
c)
TTG
AJM4
AJM5b
Age = 3539±220 Ma
Initial 176Hf/177Hf =0.280687±0.000035
MSWD = 8.9
n=4
176Hf/177Hf
176Lu/177Hf
d)
TTG
Age = 2661±760 Ma
Initial 143Nd/144Nd =0.50884±0.00048
MSWD = 23
n=6
143Nd/144Nd
147Sm/144Nd
e)
Gabbronorites
Age = 3225±1400 Ma
Initial 176Hf/177Hf =0,28082±0.00084
MSWD = 21
n=4
176Hf/177Hf
176Lu/177Hf
f)
Gabbronorites
Age = 3324±1300 Ma
Initial 143Nd/144Nd =0,5083±0.0017
MSWD = 14
n=4
143 Nd/144 Nd
147Sm/144Nd
Charnockites
Granodiorites
TTG gneisses
Gabbronorites

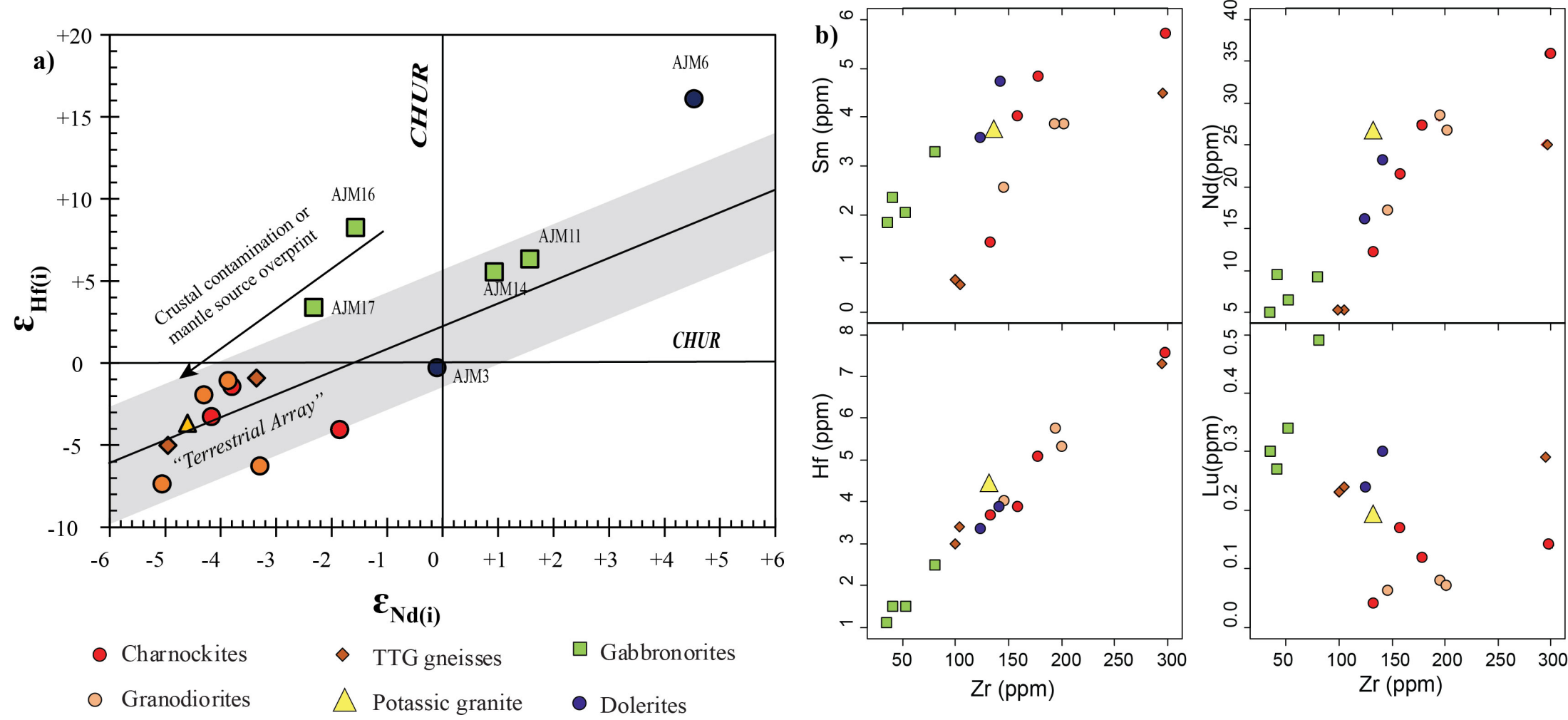
a)
b)
CHUR
CHUR
AJM6
AJM16
AJM11
AJM14
AJM17
AJM3
Crustal contamination or mantle source overprint
"Terrestrial Array"
$\varepsilon_{Hf(i)}$
$\varepsilon_{Nd(i)}$
Charnockites
TTG gneisses
Gabbronorites
Granodiorites
Potassic granite
Dolerites
Sm (ppm)
Nd(ppm)
Hf (ppm)
Lu(ppm)
Zr (ppm)
Zr (ppm)

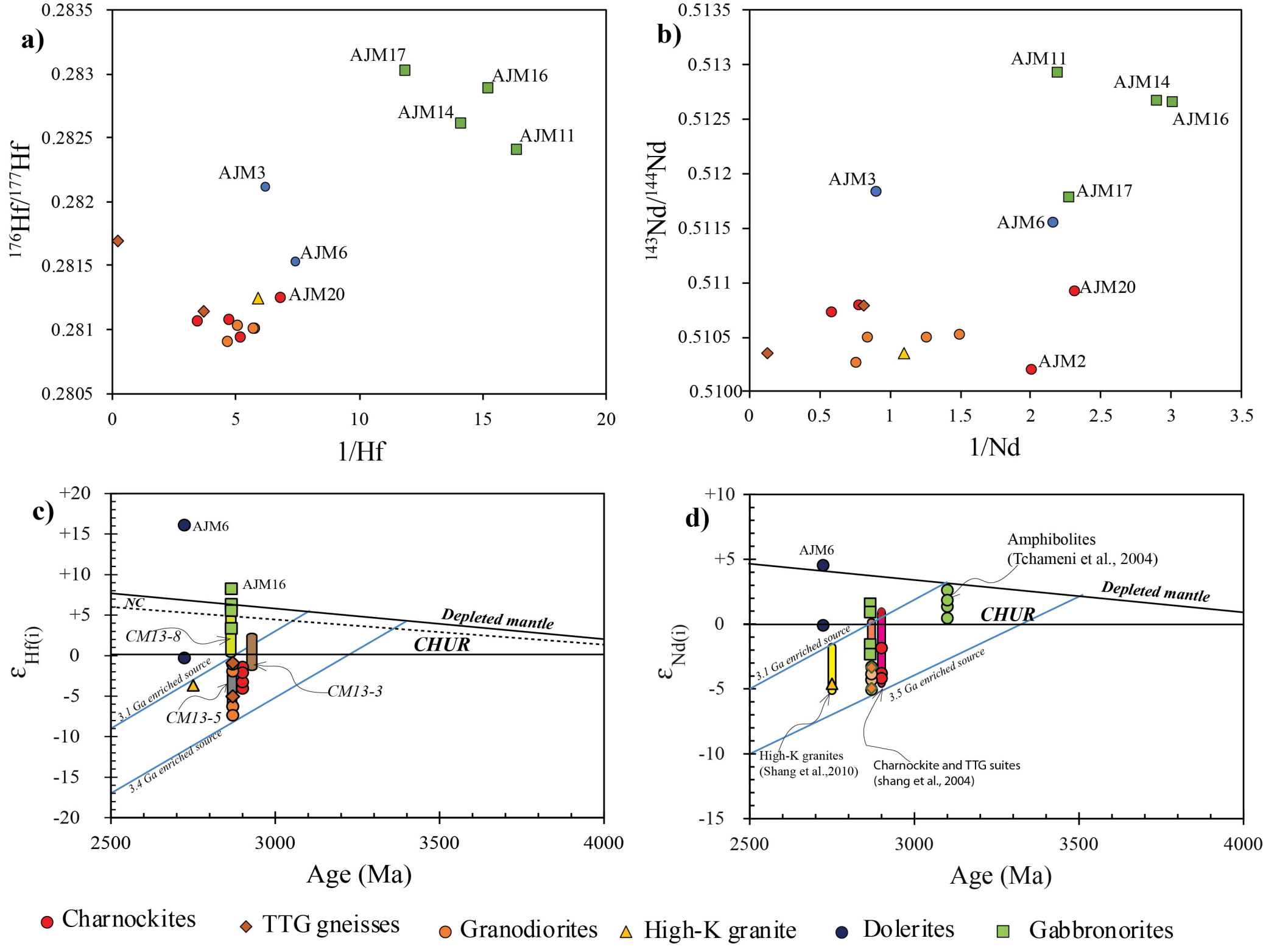
a)
$^{176}Hf/^{177}Hf$
1/Hf
AJM17
AJM16
AJM14
AJM11
AJM3
AJM6
AJM20
b)
$^{143}Nd/^{144}Nd$
1/Nd
AJM11
AJM14
AJM16
AJM3
AJM17
AJM6
AJM20
AJM2
c)
$\varepsilon_{Hf(i)}$
Age (Ma)
AJM6
AJM16
NC
Depleted mantle
CHUR
CM13-8
CM13-3
CM13-5
3.1 Ga enriched source
3.4 Ga enriched source
d)
$\varepsilon_{Nd(i)}$
Age (Ma)
AJM6
Amphibolites
(Tchameni et al., 2004)
Depleted mantle
CHUR
3.1 Ga enriched source
3.5 Ga enriched source
High-K granites
(Shang et al.,2010)
Charnockite and TTG suites
(shang et al., 2004)
Charnockites
TTG gneisses
Granodiorites
High-K granite
Dolerites
Gabbronorites

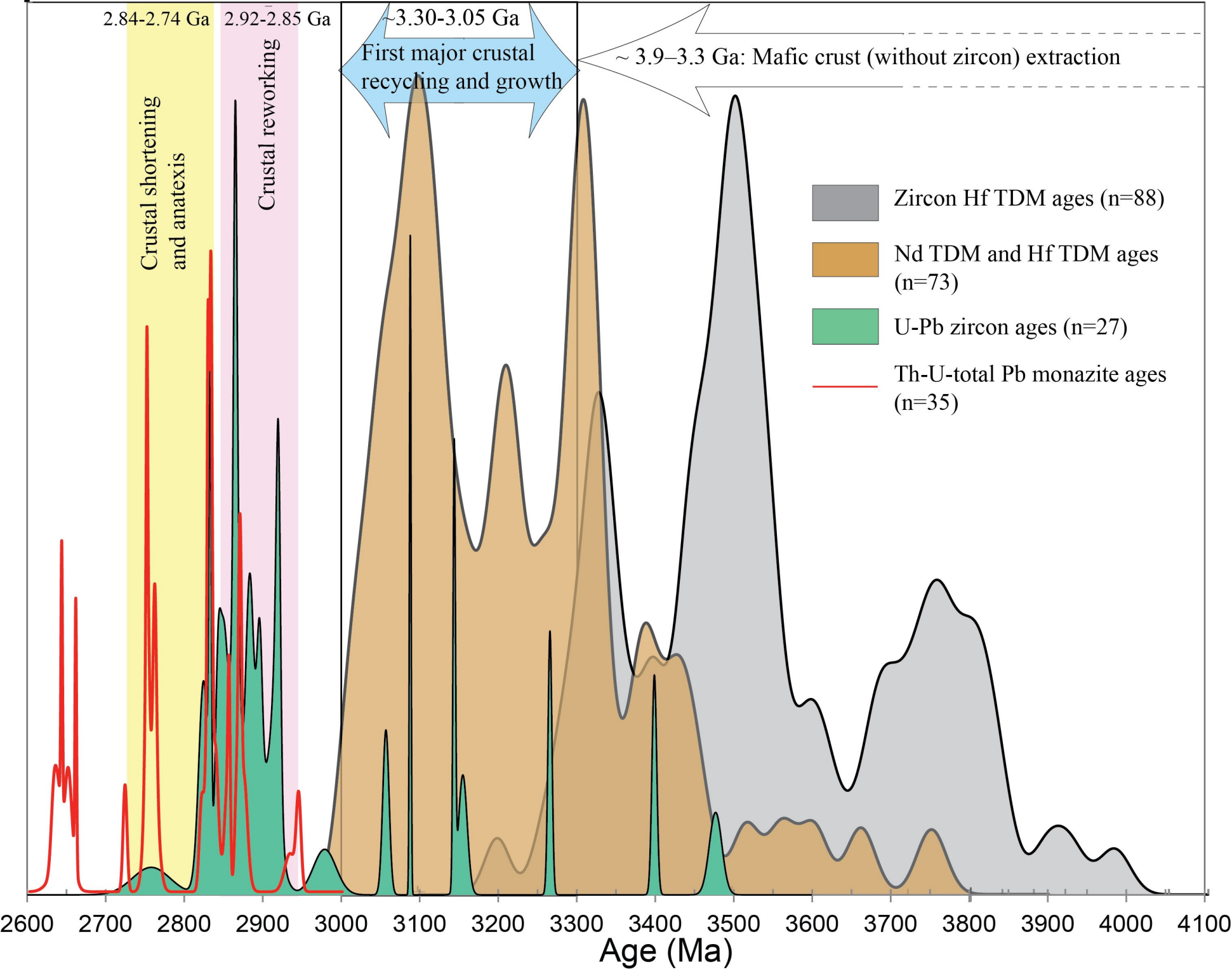
2.84-2.74 Ga
2.92-2.85 Ga
~3.30-3.05 Ga
First major crustal recycling and growth
~ 3.9–3.3 Ga: Mafic crust (without zircon) extraction
Crustal shortening and anatexis
Crustal reworking
Zircon Hf TDM ages (n=88)
Nd TDM and Hf TDM ages (n=73)
U-Pb zircon ages (n=27)
Th-U-total Pb monazite ages (n=35)
2600
2700
2800
2900
3000
3100
3200
3300
3400
3500
3600
3700
3800
3900
4000
4100
Age (Ma)